Stockholm University

Bachelor Thesis

Degree Project in
Geology 30 hp

Garnet porphyroblast growth in a possible layered igneous intrusion, Rimbo, Sweden

Mikaela Lindström

Stockholm 2021

Department of Geological Sciences
Stockholm University
SE-106 91 Stockholm

Acknowledgments

First and foremost, I would like to thank my supervisor Professor Alasdair Skelton for his guidance and valuable input throughout the fieldwork and writing of this thesis. Furthermore, I would like to thank my partner, Jonatan Cairenius, for his encouragement and company during the fieldwork. Last but not least, I would like to thank my family for their endless support.

Abstract

In recent years, a former layered igneous intrusion hosting anomalously large garnets was discovered near Rimbo, Sweden. The intrusion is visible in 6 outcrops, which have been analysed and discussed in this study. The igneous intrusion containing the garnets has undergone metamorphism at amphibolite conditions. The garnets occur in three of the outcrops and the largest garnets are approximately 11cm in diameter. In this study, the outcrops were chemically analysed in the field using a handheld X-ray fluorescent (XRF) analyser. Rock samples were retrieved from all localities and they were used for a petrographic analysis. It was found that the outcrops mainly consist of plagioclase, hornblende, biotite and quartz, and that the anomalously large garnets exhibit compositional zoning. The conclusions reached in this study were that the host rocks most likely represent a former layered igneous intrusion and that the reason for occurrence of the large garnets could not be established.

Keywords: garnet, porphyroblast, mafic intrusion, XRF-analysis, compositional zoning

Sammanfattning

För några år sedan upptäcktes en lagrad magmatisk intrusion med ovanligt stora porfyroblaster av granatkristaller utanför Rimbo, norr om Stockholm. Den magmatiska intrusionen analyseras i 6 lokaler som har genomgått metamorfos i amfibolit facies. Granater förekommer i tre av lokalerna och de största uppmätta granaterna i området är ungefär 11cm i diameter. I denna studie har dessa lokaler blivit analyserade i fält med hjälp av en XRF-röntgen. Vid varje lokal togs prover som sedan användes för att tillverka tunnslip och som sedan studerades i en petrografisk analys. Resultaten visade att de mineral som huvudsakligen förekommer i intrusionen är plagioklas, hornblende, biotit och kvarts samt att de stora granaterna har zonering. Slutsatserna av studien var att lokalerna troligtvis är en del av en metamorfoserad lagrad mafisk intrusion och att mekanismen för tillväxt av de stora granaterna inte kunde bestämmas.

Nyckelord: granat, porfyroblast, mafisk intrusion, XRF-analys, zonering

Table of Contents

1 Introduction

Garnets are an important group of minerals for constraining metamorphic conditions, by providing information about the P-T path for medium to high grade metamorphic rocks [Mezger et al., 1992]. Therefore, a garnet-bearing metamorphic rock can be studied in order to investigate the metamorphic history of an outcrop. Garnets are common metamorphic rock-forming minerals and since they are high in the crystalloblastic series, it is not uncommon for them to grow as porphyroblasts. However, in a handful of locations in the world, garnet porphyroblasts have grown anomalously large.

In Gore Mountain, New York, the largest garnet crystal has been measured to 1m in diameter [Kelly, 1992]. The process of formation of anomalously large garnet crystals is poorly understood, although several hypotheses have been proposed [Hartung et al., 2020]. Recently, a possible layered mafic intrusion hosting anomalously large garnets was discovered near Rimbo, Sweden (fig. 1). The intrusion is observed in 6 outcrops (A to F) which are hypothesised to represent different stages of the intrusion. Three of the outcrops (A to C) contain visible garnet crystals, and at locality A the garnets are anomalously large.

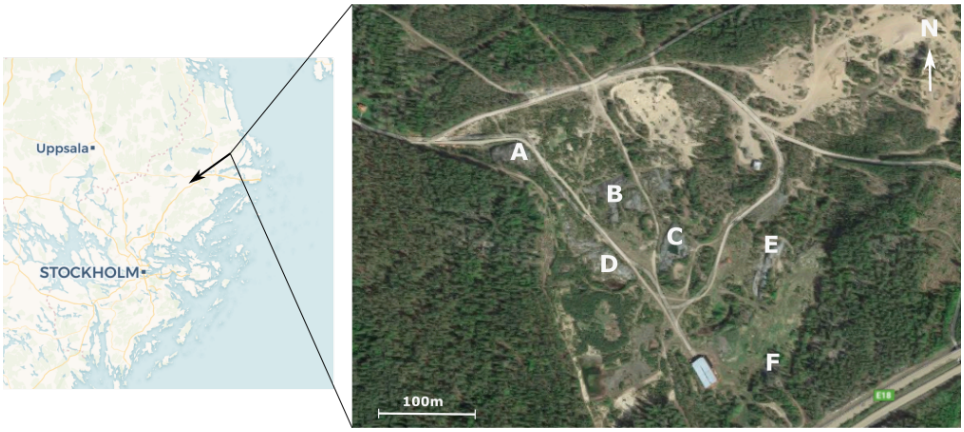

Figure 1: *The area of interest is located in a sand quarry near Rimbo, 60km NE of Stockholm, and consists of 6 outcrops (A to F) with varying features and characteristics.*

Layered mafic intrusions are large rock bodies consisting of mafic minerals which intruded at depth in the Earth [Cawthorn, 2020]. These intrusions may have compositional layering, which can be indicative for the base of a magma chamber [Ferré et al., 2009]. However, it is important to study the mineral assemblages in the intrusion in order to understand the magma system from which it has crystallised [Zhang et al., 2020]. An igneous intrusion is typically most mafic in the bottom and becomes increasingly felsic

towards the top. It may undergo metamorphism and form a successive series of metamorphic rocks depending on the amount of mafic minerals in the protolith. A petrographic analysis provides information about the mineral assemblages which, together with mineral reaction structures, holds important clues in the investigation of metamorphic history and possible parental magma.

In this study, the outcrops near Rimbo, Sweden, will be investigated in the field and a petrographic analysis will be conducted in order to characterize the rocks. To progress in the study of unusually large garnet porphyroblasts, it is vital to study nearby rocks in which they are not hosted, aiming to find the key difference. The aim of this study are to test the hypotheses that the outcrops near Rimbo represent parts of a layered igneous intrusion and to find the reason for occurrence of large garnets.

2 Geological setting

This study is centered around a recently discovered area of geological interest near Rimbo, Sweden (fig. 1). The study area is part of the Svecofennian Province, which consists of metamorphosed sedimentary and volcanic rocks [Lundqvist and Bygghammar, 1994]. Generally, the rocks are 2000-1800 million years old [Wahlgren and Schoning, 2018]. The province includes more than half of Sweden's bedrock surface and stretches from south of the Stockholm area to the north of Sweden [Andréasson, 2015]. In the Svecofennian Province, volcanic rocks are commonly silica-rich, implying acidic parental magma, and the occurrence of acidic volcanic rocks is often coupled with ore deposits.

In the Stockholm area, there are large-scale antiforms and synforms which stretch for several kilometers. These structures indicate plastic deformation which has had a great affect on the geological evolution [Wahlgren and Schoning, 2018]. The Norrtälje-synform is located close to the study area and it is connected to the Värmdö-antiform to the south. The antiform-synform pattern is compressed in a N-S direction, indicating shortening.

The study area consists of 6 outcrops (A to F) with varying features and characteristics (fig. 1). According to existing geological survey data, obtained from the database of the Geological Survey of Sweden, the bedrock geology in the study area consists of a gneissic ultrabasic to basic intrusive rock (fig. 2). North of the outcrops, there is a brittle zone of deformation, which could be a fault or a fracture zone. The surrounding area consists of different types of acidic intrusive rocks, of which some are porphyritic, which is consistent with the general bedrock geology of the Svecofennian Province.

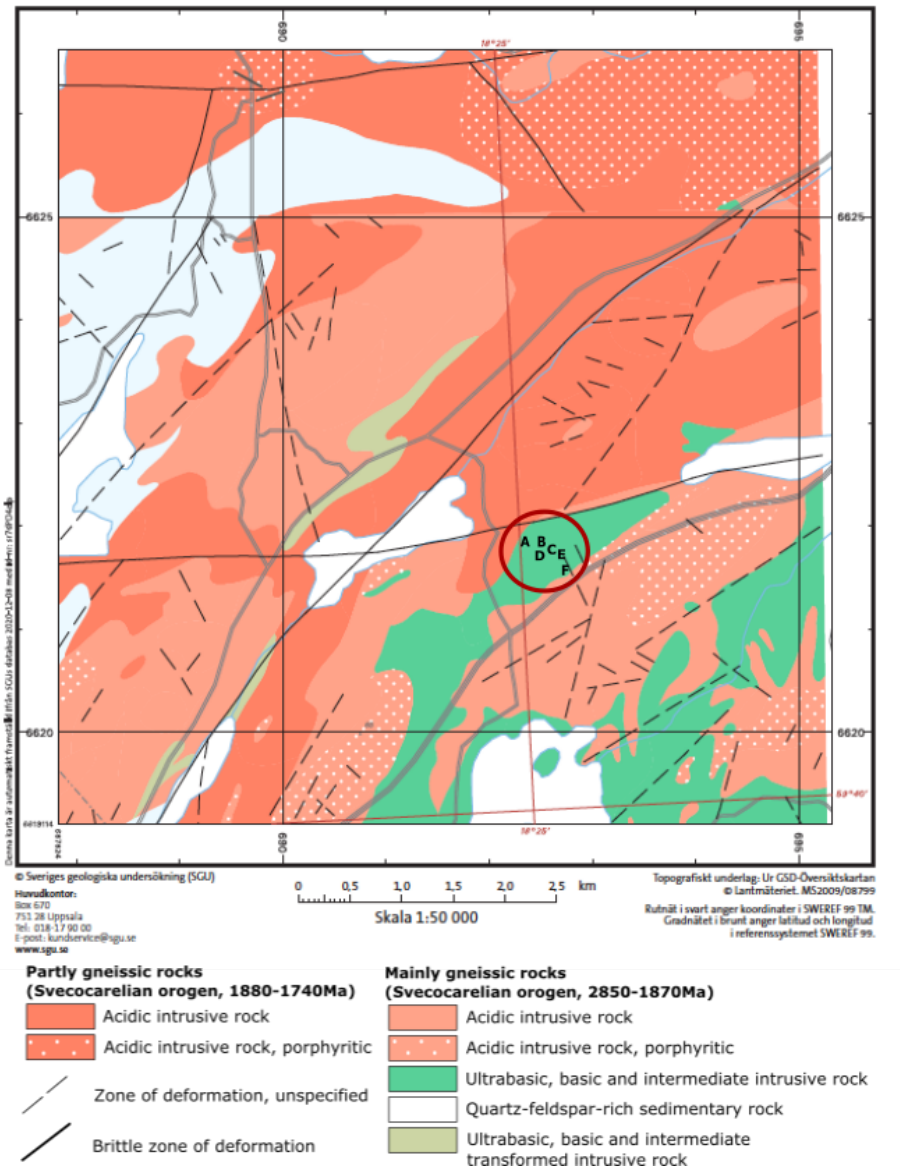

Figure 2: *The map shows the bedrock geology from the study area and the surrounding area. All of the localities are located on an ultrabasic, basic and intermediate intrusive rock, while the surrounding area is characterized by acidic rocks. Locality E and F are located close to a zone of deformation. The bedrock map was obtained from the Geological Survey of Sweden (SGU).*

The outcrops were found by paleontologist Johan Dalsätt in 2018, and they were first described by geologists Åke Johansson, Risto Kumpulainen and Nina Rantakokko [Johansson et al., 2018]. They identified locality A to be a silica-poor plutonic rock that has undergone deformation and metamorphism. Furthermore, they concluded that the rock is most likely a migmatitic amphibolite and proposed that the amphibolite is possibly located in a fold which could permit metamorphic fluids to collect allowing formation of the large garnets. Possible igneous layering at locality A was also identified. They also observed that the garnets only occur in one specific area and do not occur in all outcrops.

3 Scientific background

3.1 Previous research of garnets

Garnets are a group of silicate minerals with the general formula $X_3Y_2(SiO_4)_3$. Garnet end member phases can be divided into two main groups, the pyralspite group consisting of pyrope, almandine and spessartine, and the ugrandite group consisting of grossular, andradite and uvarovite [Klein and Philpotts, 2017]. There is solid solution within the two main groups which yields various possible chemical compositions in naturally occurring garnets.

Different species of garnet crystallize at different temperatures which produces chemical zoning from core to rim [Atherton, 1968]. Generally, the weight percent (wt.%) almandine and pyrope increases while the wt.% spessartine and grossular decreases with increasing metamorphic grade. As a result, a Mn-rich core with an Mn-poor rim is produced, indicating prograde growth of garnet. The chemical profile which develops is considered a classical bell-shaped pattern [Atherton, 1968, Tracy et al., 1976]. Compositional zoning is essentially a record of crystallisation history and therefore, the property of zoning makes garnets suitable for geothermobarometry [Ferry and Spear, 1978].

Hartung et al. [2020] studied garnet porphyroblasts in the Passos Nappe, Brazil, and their results showed that the garnets had chemical zoning with decreasing amount of spessartine and grossular from core to rim, while the amount of pyrope and almandine was increasing. They concluded that the smaller garnet crystals displayed the same zoning pattern as the larger garnet porphyroblasts, indicating a shared evolution. Chemical zoning in garnets often show a weak trend of increase of spessartine and almandine in the outermost rim, most likely due to diffusion of Fe-Mg with the matrix during retrograde metamorphism [Spear and Florence, 1992]. Compositional zoning is an indicator of garnet growth history and timing in relation to other metamorphic events.

In order to acknowledge the processes that control anomalous growth of garnet, it is necessary to understand the mechanisms that govern porphyroblast and crystal growth. There are essentially two processes responsible for crystal formation in metamorphic rocks: nucleation and growth [Philpotts and Ague, 2009]. Nucleation provides nuclei on which growth can initialise and the growth process needs influx of nutrients to progress. During crystal growth, diffusion allows elements to be transported to and from the crystal interface. From these two processes, it is evident that during formation of porphyroblasts, growth is favoured over nucleation.

Studies have shown a linkage between matrix microstructures and porphyroblast growth [Stallard and Hickey, 2002]. For example, it has been suggested that deformational microstructures, such as crenulation cleavages, are favourable environments for growth and nucleation of porphyroblasts [Williams, 1994]. Stallard [1998] studied garnet porphyroblast growth and its linkage to microstructures in the Fleur de Lys Supergroup, Newfoundland, and found that even porphyroblasts that are close in proximity may have internal structures that indicate different petrogenetic histories, despite that they likely have experienced identical P-T conditions. Therefore, a combination of microstructures, P-T conditions and bulk composition of the host rock were introduced as an explanation of the variation. The microstructures of interest are mainly foliation, both within the porphyroblast and the matrix, and crenulation cleavages [Stallard and Hickey, 2002, Williams, 1994].

In previous research, the occurrence of extraordinarily large garnets has been attributed to influx of metamorphic fluids [Goldblum and Hill, 1992]. At Gore Mountain, New York, the largest known garnets have been found, some have been measured to 1m in diameter [Kelly, 1992]. There are megacrystic garnets occurring in several places in the Adirondack Mountains, but none as large as the ones at Gore Mountain. McLelland and Selleck [2011] proposes that the garnets at Gore Mountain have grown large as a result of interaction between fluids and gabbroic rocks at upper amphibolite facies. They go on to state that the presence of fluids under mid-crustal temperatures and pressure is peculiar, and they suggest that fluids were introduced through a fault which passes by Gore Mountain. Adjacent to the garnet ore zone, there are feldspar-rich rocks which under amphibolite-facies temperatures deform plastically, whereas the garnet-bearing mafic rocks deform by brittle processes [Goldblum and Hill, 1992]. The juxtaposition of two rock bodies of different plastic strength produces high strain rates, which causes fracturing of the brittle rock body. These fractures could provide a way for fluids to enter the mafic rock and in turn, aid the growth of megacrystic garnets.

In order to understand the occurrence of anomalously large garnets, it is vital to understand the constraints of growth. Spiess and Bell [1996] studied gar-

net zonation from the Meran-Mauls basement in South Tyrol and suggested that the termination of porphyroblast growth is controlled by termination of access to material due to intensified foliation of the matrix. Consequently, the growth of a strain shadow may eventually cause porphyroblast growth to cease. [Bell et al., 1986] proposed that porphyroblast growth is restricted by progressive shearing which occurs at the edges of a grain parallell to the foliation. The proposal is based on observations that porphyroblast growth cannot persist at sites of active shearing.

3.2 Evolution of layered mafic intrusions

Mafic intrusions often display a geochemical and mineralogical layering which is attributed to differentiation processes in a magma chamber [Ferré et al., 2009]. The scale of these layers vary from a few centimeters to hundreds of meters. They consist of a succession of layers generally characterized by change in grain size and mineral composition [Namur et al., 2015]. In addition, igneous layering can have varying thickness and orientation within the same mafic intrusion. In general, mafic intrusions are characterized by ultramafic rocks at the base, followed by a layered series and iron-enriched intermediate units at the top [Ferré et al., 2009].

There are a number of large layered igneous complexes that have been described over the years. One of them is the Skaergaard intrusion, which is located on Eastern Greenland. The Skaergaard intrusion can be divided into three distinct groups; the marginal border group, a layered series and the upper border group [Philpotts and Ague, 2009]. These groups represent a continuous evolution from primitive olivine gabbro to quartz-ferrodiorite [Larsen and Tegner, 2006]. The Skaergaard intrusion formed by a single pulse of magma and the layered series consists of gabbroic rocks [Larsen and Tegner, 2006]. On the other hand, another layered intrusion, the Muskox intrusion in Canada, consists of 25 cyclic units which each formed by fractional crystallisation of a new batch of magma [Philpotts and Ague, 2009]. The continuous influx of new magma allows for more olivine-rich layering to form, because the residual is exchanged to new perioditic magma.

Pons et al. [2006] studied the Tarçouate Laccolith, Morocco, to find its whole-rock chemistry and to investigate the development of igneous layering during its growth. They found that the pluton consisted of three magma batches, muscovite granite, biotite granodiorite and finally hornblende granodiorite accompanied by monzodiorite. The magma series becomes increasingly more mafic and the igneous layering was found in the most mafic part of the pluton.

The mechanism which controls crystallisation in a magma chamber is still under debate. The two main theories are that layers form by crystal settling,

abiding the law of gravity, or that magma crystallises against the floor and the walls of the chamber [Martin, 1990]. It is most likely that the development of igneous layering cannot be attributed to a single crystallisation process, but it is suggested that the majority of crystallisation occurs in situ on the margins of the magma chamber [Namur et al., 2015]. However, the flow and movement of magma itself also controls the development of igneous layering. Layering can form as a result of injection and extraction of magma to and from the magma chamber [Ferré et al., 2009]. In addition, layering may develop while influx of magma is continuous or from a single batch of magma. The result will differ because influx of new magma allows the layering to be more perioditic in composition. On the contrary, layering evolved from a single batch of magma will become increasingly felsic across the whole intrusion as the mafic minerals settle out.

4 Method

4.1 Fieldwork

The fieldwork was conducted during the periods: 28-30/10 and 4-6/11 2020. Each site (A to F) was described geologically both with attention to details and to larger-scale features. At localities A to C, a $1m^2$ square was constructed and the garnet crystals within were counted and their diameters were measured. The chemical analysis was conducted using an Olympus DELTA (model DP-6000) X-ray fluorescent (XRF) analyser. The analyser emits an X-ray beam which has enough energy to affect the electrons of the inner shells of elements. As the beam hits an electron, it is knocked out of place which causes the atom to become unstable. As a consequence, electrons from the outer shells are moved up a shell until all orbitals are filled. When electrons move from an outer shell to an inner shell, energy is lost and the amount of lost energy is specific to each element. Hence, the lost energy can be used by the XRF analyser to calculate which element the X-ray beam hit. The locations for chemical analysis were randomly chosen at each site with the aim of spreading the sampling across the whole outcrop in order to get representative results.

The chemical analysis was focused on three main features of the localities; the chemical composition of the country rock as a reference, the chemical composition of garnet crystals and the chemical composition of alterations in the country rock. At each locality, the type of chemical analysis that was conducted depended on the features present in the outcrop. As a consequence of the variability between the outcrops, the methodology had to adapt specifically to each locality.

Prior to conducting the analysis in the field, the localities were investigated to observe what type of features the outcrops contained. The chemical anal-

ysis of the country rock was conducted at all localities and 25 measurements were made. The method and amount of measurements of garnets and alterations were adapted for each locality due to the variability. At locality A, the garnet crystals were large enough to measure cross-sections which allows investigation of chemical zoning. Hence, cross-sections across 15 garnet crystals were measured. Locality A also contains no alterations but shows evidence of igneous layering. As a consequence, a cross-section of 60 cm was measured along the possible igneous layering to examine if the contacts between the layers are gradual or sharp. Sharp contacts are indicative of gneissose banding, whereas gradual contacts indicate pre-metamorphic igneous layering.

Locality B contains garnet crystals and alterations. However, the garnet crystals are not large enough to allow cross-sections to be measured. Therefore, 25 measurements of garnet crystals was done, aiming to measure as close to the center of the garnet crystals as possible. The chemical composition of the alterations were measured as cross-sections of 11 cm across the alteration and 5 cross-sections were measured. Locality C has the same features as locality B, therefore the analysis was conducted using identical methodology.

At locality D, there are no garnets present and very few alterations were found. Hence, 2 cross-sections of 11 cm were measured across alterations. Locality E does not contain any garnets, but there are plenty of alterations. Therefore, 5 cross-sections of 11 cm were measured across alterations. Finally, locality F has similar features as locality D, hence the same methodology was used.

4.2 Laboratory work

In the laboratory, the samples were cut with a diamond saw and prepared for thin sections. The samples were packaged and sent to Vancouver Petrographics where they were prepared as thin sections. In total, 20 thin sections were made. Petromicrographs were taken using a Nikon Optiphot2-pol microscope with associated camera software. The thin sections were studied using a Leica DMLSP polarized light microscope. The point counting was conducted using a Pelcon Automatic Point Counter, with the software PelconPointCounter9 v2.00. The steplength 0.5mm was used. Ideally when point counting, each point should be located on a new crystal. Hence, judging by the crystal sizes in the thin sections produced in this study, it was suitable to use 0.5mm. For each thin section, 500 points were counted. The standard error of point counting was calculated using equation (1) the following equation which was presented by Plas and Tobi [1965] where X is the points counted for each mineral.

$$SE = 2 * \sqrt{\frac{(\frac{X\%}{100-X\%})}{500}} \tag{1}$$

The percent of anorthite in the thin sections were determined using the Michel-Levy method. In this method, the percent of anorthite is determined by first locating the (010) planes on plagioclase crystals. By turning the stage the maximum extinction angles for the twin pairs are found (fig. 3). The difference between the middle angle when neither twin pair is in extinction and the left and right angles were noted. A 5° difference between the left and right twinning extinction angles was allowed. In each thin section, as many plagioclase crystals as possible were used with the aim to obtain at least 5 maximum extinction angles for each locality. Finally, the percent of anorthite is determined by using the Michel-Levy chart, provided in appendix A.

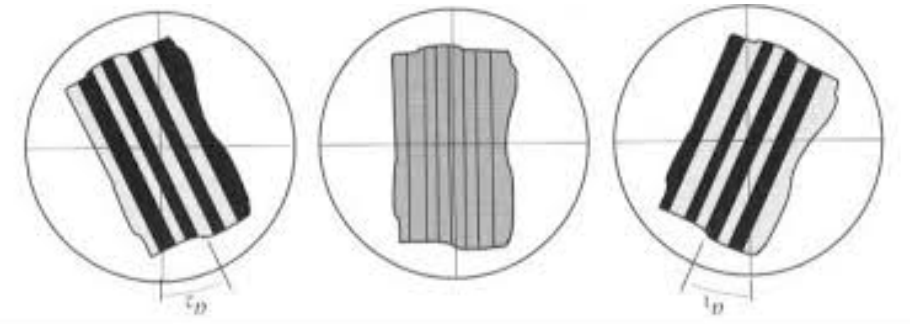

Figure 3: *By turning the stage the maximum extinction angles can be located.*

4.3 Data processing

The data obtained from the XRF-analyser during the fieldwork was processed using Microsoft Excel v16.43 (MS Excel). The analyser registered both the percent of element and the respective standard error of measurement. However, due to technical limitations, the lighter elements are not detected by the XRF-analyser. These elements are registered as LE (Light Elements). As a consequence, data collected from an XRF-analyser in the field with high LE values cannot be presented as volume percent (vol.%) element of the whole sample. Therefore, ratios of the elements are used. Ratios will accurately represent the chemistry of the outcrops because even though there are high LE values, the ratios of the heavier elements are true.

It was expected that locality A to F would become increasingly felsic, therefore the ratio Fe/Si was used to compare the host rocks. The average was

calculated from the 25 measurements and the standard deviation was calculated using the formulas in MS Excel. The cross-sections of the large garnets were compared using the sum of Ca, Mg, Fe and Mn as the denominator since these are the four main elements that characterize different garnet species. Each of these four elements were compared in a ratio with the sum. The average amount of Mn in the smaller garnets were calculated the same way. Averages of the 15 garnets were calculated for each element from core to rim in order to do a general overview of the change of elements. These averages were calculated by using the mid-value of each garnet for the core average and the two end-values of each garnet for the rim average. In the garnets with two mid-values, hence an even number of measurements, the averages between those were used for the core average.

The data of the igneous layering was processed by comparing the change of Si, Fe and Ca across the alterations. These elements were compared in a ratio with (100-LE) as the denominator. (100-LE) is used because it subtracts the elements that could not be detected by the XRF-analyser. Hence, the element of interest is only presented as a ratio with the elements that could be distinguished by the analyser. The alterations were analysed by trying several different ratios with Si as the denominator aiming to find a pattern of change in the cross-section. Eventually, the ratio K/Si was used to analyse the alterations because there was a clear pattern in relation to the change of Si.

5 Results

5.1 Geological description

5.1.1 Locality A

The outcrop is located at 59°41'24.495"N, 18°25'04.425"E and it has a dark, mafic appearance. The main feature of the outcrop are the cm- to dm-sized garnet crystals which occur in the outcrop. The diameters of the crystals varies but are around 7-11cm. However, garnet crystals also appear in the matrix of the country rock and these garnets are much smaller. The garnets are not uniformly distributed but rather occur in clusters. Garnets are eu- to subhedral and dark red to brown in colour. There is a depletion halo of quartz, creating a strain shadow, that surrounds the garnet crystals.

In the country rock, there is a metamorphic foliation in a NE-SW orientation, which coincides with the strain shadows of the garnet crystals. There is a vein in the outcrop that is white to gray in colour and occurs with no specific orientation pattern. The vein has clear crystals and has no chill margin or baked contact. On the west side of the outcrop, there is possible igneous layering. The layers are alternating darker and thinner as well as

Figure 4: *The possible igneous layering is characterized by alternating darker and lighter layers. There are garnet porphyroblasts occurring in the possible igneous layering. The geological hammer is 50cm.*

lighter and thicker (fig. 4). It is not possible to observe in the field if the variation is gradual or sharp because the outcrop is overgrown by moss. The possible layering contains both large and small garnet crystals. The occurrence of garnet crystals in the possible layering does not form a pattern but appears randomly. Furthermore, there are a few alterations that are white to pink in colour which occur along very fine cracks with no specific orientation pattern. Within a 1 m^2 area, 16 garnets occurred with an average diameter of 8.8cm.

5.1.2 Locality B

The outcrop is located at 59°41'22.623"N, 18°25'13.103"E. It has a dark, mafic appearance. In the outcrop, there is a strong metamorphic foliation in a SW-NE orientation. The outcrop contains garnet crystals that are euto subhedral and dark red to brown in colour. The garnets occur in the central and north parth of the outcrop and appear in clusters rather than being uniformly distributed. Commonly, the garnet crystals are around 1cm in diameter. However, the diameter of the garnets vary in the outcrop but within the same cluster, the size appears relatively uniform. There is no visible rim of quartz around the garnet crystals.

The outcrop has many intrusions and alterations, mostly occurring in a SW-NE orientation, meaning that they are parallell to the foliation. There are both darker, more mafic intrusions and lighter, more felsic intrusions. In the central part of the outcrop, there is a large pink coloured intrusion, which is 30 cm at its widest (fig. 5b). The crystals in this intrusion are clearly visible. This intrusion does not occur in a specific orientation pattern as opposed to the other intrusions in the outcrop. At the edge of the outcrop, there are lenses of a dark, coarse-grained fill (fig. 5a). There is evidence of displacement in the outcrop, which is especially visible close to the pink intrusion. At the south part of the outcrop, the rock is significantly more weathered and the outcrop appears granulated. Within a $1m^2$ area, 156 garnets occurred, which were approximately 1cm in diameter.

(a) A 'lense' (b) A felsic pigmatitic intrusion

Figure 5: *Locality B contains several features. The geological hammer is 50cm.*

5.1.3 Locality C

The outcrop is located at 59°41'20.732"N, 18°25'19.462"E. It has a dark, mafic appearance. The outcrop contains garnets crystals that are eu- to subhedral and dark red to brown in colour. The crystals vary in size, where the largest garnets are up to 3cm in diameter. The garnets are overall randomly distributed and vary greatly in size from one part of the outcrop to another. Most of the garnet crystals are surrounded by a depletion halo of quartz, however, there are garnets that do not display this feature.

The outcrop has several alterations which appear as white to pink, felsic strings across the outcrop (fig. 6b). They show no systematic orientation and occur both on undamaged parts of the outcrop and along cracks. In some locations, the alterations are more white and appear very fine-grained but commonly they appear as a change in colour compared to the country rock, meaning that the grain size has not changed. There is also a pink coloured intrusion of which has clear visible crystals and there is no chill margin or baked contact. On other parts of the outcrop there are other in-

trusions which are darker and more mafic. On the south side of the outcrop, there is evidence of displacement in a NW-SE direction (fig. 6a). Within a $1m^2$ area, 58 garnets occurred, that were between 1.5-2cm.

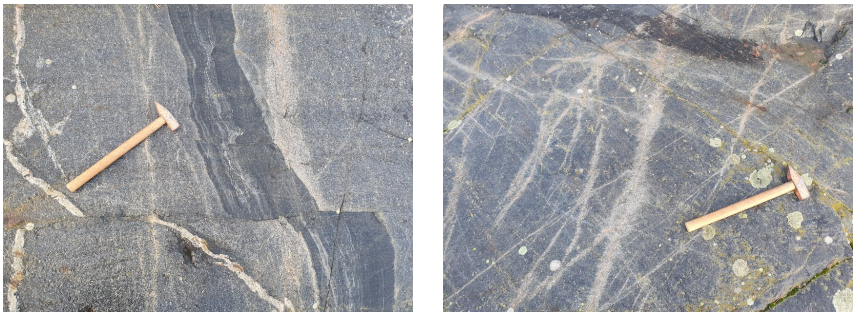

(a) Evidence of displacement (b) Alterations in the outcrop

Figure 6: *Locality C contains several features. The geological hammer is 50cm.*

5.1.4 Locality D

The outcrop is located at 59°41'19.017"N, 18°25'14.421"E and overall has a dark, mafic appearance. When observing the outcrop closely, the colour of the country rock is found to be slightly darker further south. The outcrop is elongated and partially covered with vegetation. On the north side of the outcrop there is an area that is more felsic than the rest. There is a sharp contact with the host rock but the lighter area is quite large. The crystals are clear and visible, and the area appears "whirly", as if the rock has solidified during flowing motion (fig. 7b).

(a) A string of epidote (b) The white 'whirly' intrusion

Figure 7: *Locality D contains several features. The geological hammer is 50cm.*

On the north side of the outcrop there are several intrusions with varying characteristics. One of the intrusions contains a green, very fine-grained

rock, which is epidote-bearing (fig. 7a). Another intrusion is black and fine-grained. They do not have sharp contacts but have a gradual contact with the host rock. The outcrop has alterations which are white to pink in colour, but they are few and could only be observed in the north part of the outcrop.

5.1.5 Locality E

The outcrop is located at 59°41'19.614"N, 18°25'28.449"E. There is a metamorphic foliation, which stretches in a NE-SW orientation. There are thin, cm-sized thick white veins, which consist of quartz (fig. 8c). The quartz-filled veins are foliation parallell. Apart from the clear white veins, there are intrusions which are fine-grained and mafic, which also stretches in a NE-SW direction.

(a) A felsic intrusion

(b) Alterations in the outcrop

(c) Systematically oriented veins

Figure 8: *Locality E contains several features. The geological hammer is 50cm.*

The outcrop has a larger intrusion of pink colour which cuts across the quartz-filled veins (fig. 8a). The intrusion has large crystals in the middle and has smaller, yet still visible, crystals toward the contact with the country rock. This change in crystal size appears sharp and no baked contact or chill margin toward the country rock occurs. Below the outcrop, there is a spot where the outcrop protrudes as a separate piece from the ground which appears to be of the same composition as the pink intrusion, that has very

large crystals. Along very fine cracks, there are alterations of the rock in a white to pink colour (fig. 8b). On the north side of the outcrop there are lenses, around 1cm in diameter, of pink feldspar. They occur both in the country rock and along alterations, but are constricted to this specific part of the outcrop.

5.1.6 Locality F

The outcrop is located at 59°41'14.295"N, 18°25'27.568"E. It has a metamorphic foliation which stretches in a SW-NE direction. The outcrop has white to pink, felsic intrusions with no baked contacts to the host rock and crystals are visible in the intrusions. The intrusions are randomly oriented. There are cracks cutting vertically across the outcrop, however there is no evidence of displacement that can be observed in the outcrop. On the north side of the outcrop, there is a dark-coloured intrusion. The intrusions range in size from 2-10cm thick and do not occur in a specific orientation. There are no baked contacts with the host rock.

(a) A felsic intrusion (b) Alterations in the outcrop

Figure 9: *Locality F contains several features. The geological hammer is 50cm.*

5.2 Chemical XRF-analysis

5.2.1 Trend of the host rock

The measurements of the host rock of the outcrops show that there is statistical variation at each outcrop (fig. 10). The standard error is substantial, and as a consequence any significant change in Fe/Si ratio between localities A and C, and localities B, D, C, and F respectively, is negligible. However, it is clear that locality A and C has a significantly higher Fe/Si ratio than the other localities and are therefore more mafic. For full data see Appendix B, tables B1 to B6.

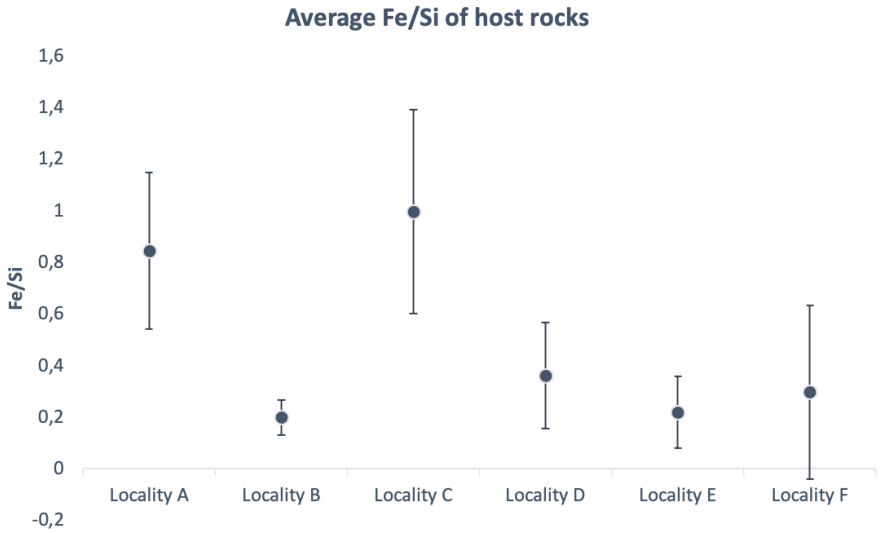

Figure 10: *The average Fe/Si ratio of the host rocks indicate that there are large margin of errors of all localities except locality B. Hence, it can only be concluded that locality A and C has a significantly higher Fe/Si ratio than the other localities.*

5.2.2 Compositional zoning of garnets

The cross-sections of garnet crystals at locality A show a clear zoning pattern of the Mn-species of garnet, spessartine (fig. 11). X_{sps} is peaking in the core of all crystals and decreasing towards the rim. The garnets vary in composition between 0.04-0.08 X_{sps}. All garnets are dominated by the Fe-species, with an average of 0.8 X_{alm}.

With calculated averages from core to rim of all 15 large garnets, it is observed that the amount of almandine, pyrope and grossular generally increases while the amount of spessartine decreases from core ($Alm_{79.6}Prp_{12.6}Grs_{11.2}Sps_{7.66}$) to rim ($Alm_{81.7}Prp_{14.9}Grs_{11.4}Sps_{5.39}$).

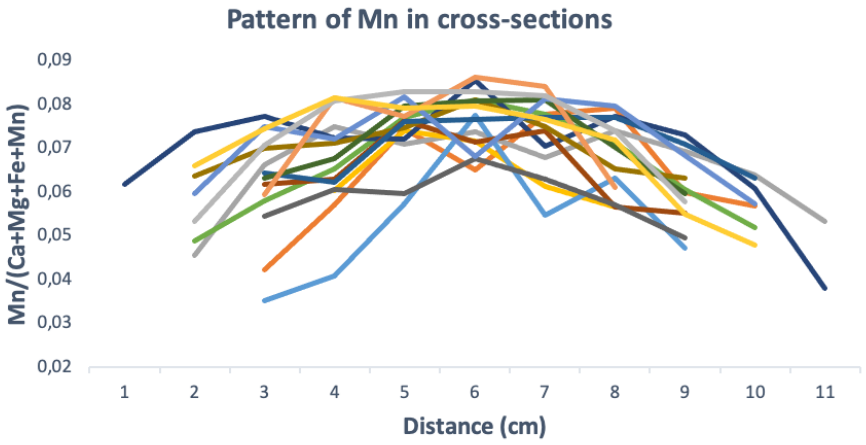

Figure 11: *The pattern of X_{sps} in the cross-sections of garnets shows a peak value of X_{sps} in the core of the crystals and a decreasing amount towards the rim. Each of the 15 lines represent one garnet.*

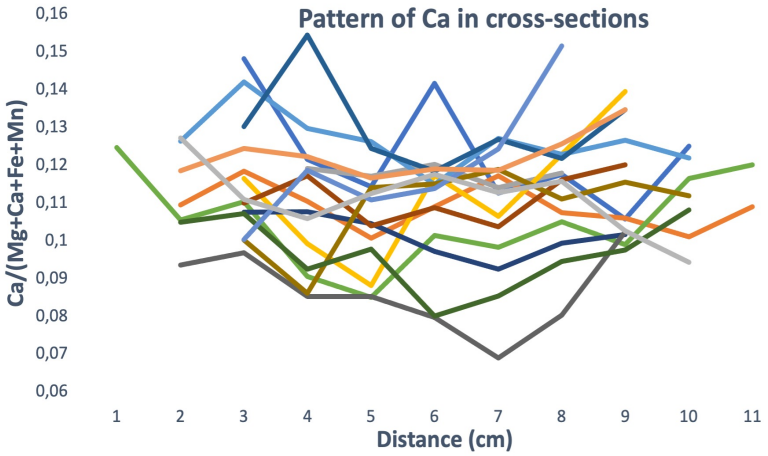

Figure 12: *The pattern of X_{grs} in the large garnets show no significant difference along the cross-section. Perhaps, a small increase towards the rim can be observed. Each of the 15 lines represent one garnet.*

Contrary to X_{sps}, the pattern of X_{grs} in the garnets shows slight increase in composition towards the rim (fig. 12). Furthermore, it can be observed that some crystals show a small decrease of X_{grs} in the outermost rim. However, many of the garnets show no change in X_{grs} along the whole cross-section.

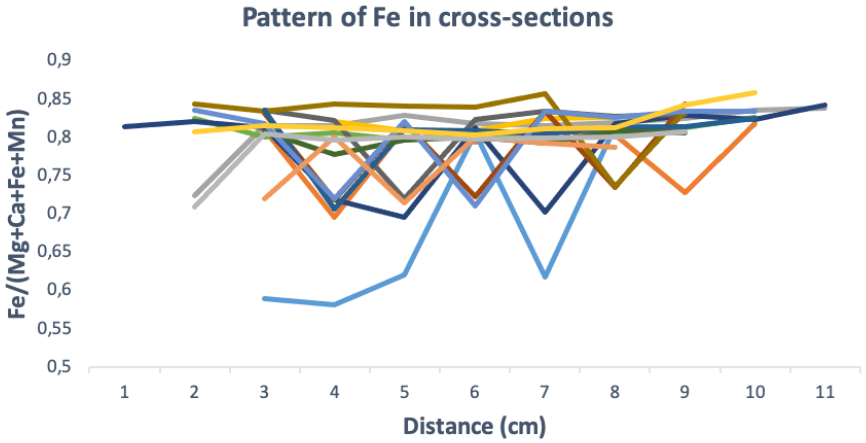

Figure 13: *The pattern of X_{alm} in the cross-sections show that there is not a significant difference in Fe in the garnet crystals. Some of the garnets have a "saw-tooth" pattern of X_{alm}. Each of the 15 lines represent one garnet.*

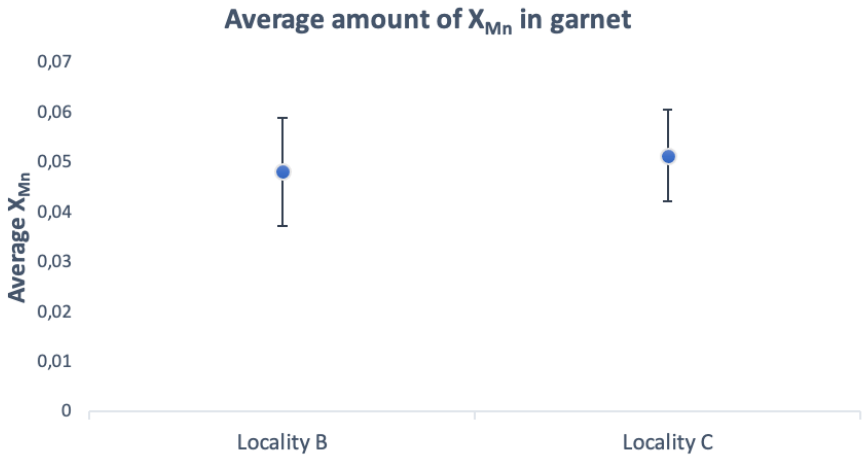

Figure 14: *The smaller garnet crystals from localities B and C show similar amounts of X_{sps} in the cores.*

The measurements of the garnets at locality B and C show that the garnets contain similar amounts of X_{sps} within the crystals (fig. 14). There are two measurements, nr 2 and 5, from locality B, that are significantly lower

in amount of X_{sps} than the other measurements. Otherwise, most of the garnets have X_{sps} of 0.03-0.06. The garnets are dominated by the Fe-species of garnet, with X_{alm} of 0.8 at both locality B and C.

In the chemical analysis, the XRF-analyser registered both "No data" and higher values (0.1-0.2) of X_{prp} in the same cross-section (see Appendix B). The XRF-analyser is not sensitive to Mg, meaning that Mg often goes undetected during analysis. Hence, it is likely the measurement of X_{prp} was obscured by dirt or another factor during the field analysis, causing the measurements to be unreliable. Consequently, the amount of X_{prp} in the garnets may be underrepresented. It must be noted, that in the samples where X_{prp} was registered, it has been taken into account to calculate the wt.% of garnet species. For full data see Appendix B, tables B7, B8 and B9.

5.2.3 Chemical variation across possible igneous layering

The 60cm cross-section of possible igneous layering displays an expected pattern of change in Si and Fe (fig. 15 & 16). Where the amount of Si peaks, at 21-23 cm and 41-43cm, the amount of Fe is at its lowest. Furthermore, the increase and decrease of Fe is gradual whereas the change in Si is sharper. The amount of Ca also peaks at 21-23cm and 41-43cm, as the amount of Si does (fig. 17). However, the increase and decrease of Ca is much more gradual than that of Si. For full data see Appendix B, table B10.

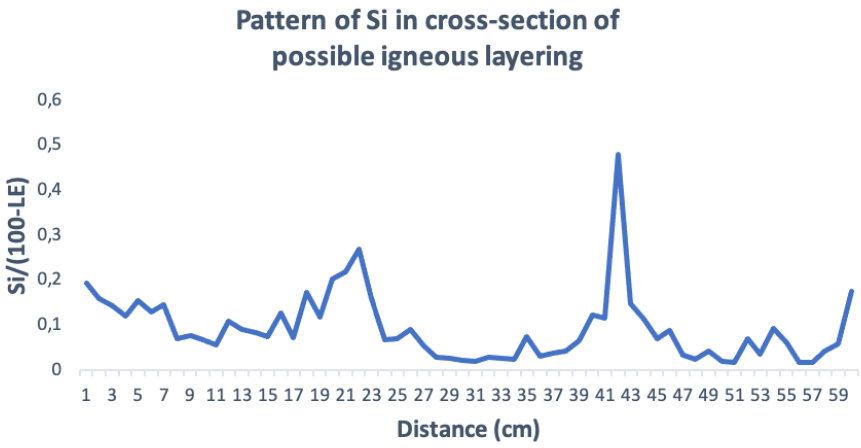

Figure 15: *Across the possible igenous layering there are peaks of the highest Si content at 21-23cm and 41-43cm. Apart from the two peaks, the amount of Si is low.*

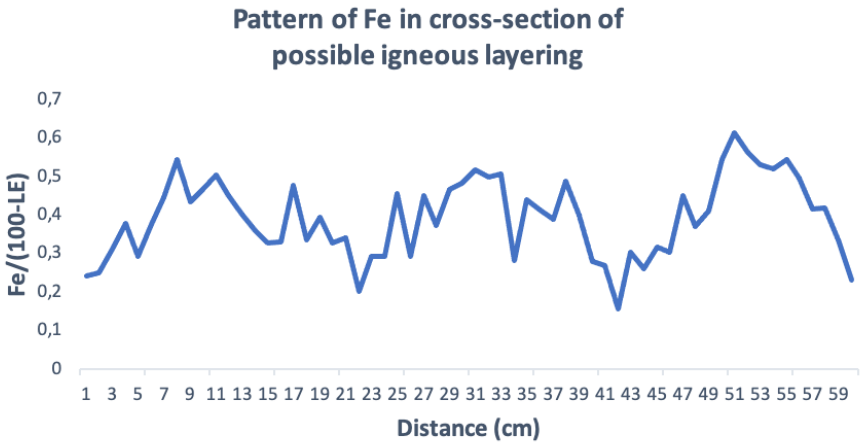

Figure 16: *Across the possible igneous layering, there are troughs in the Fe content at 21-23cm and 41-43cm. The increase and decrease of Fe is gradual.*

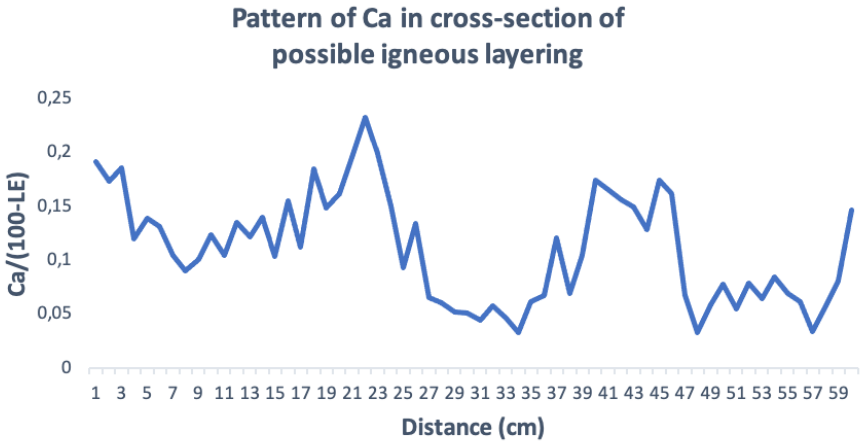

Figure 17: *Across the possible igneous layering, there are peaks in the Ca content at 21-23cm and 41-43cm.*

5.2.4 Alterations

The chemical data from the alterations indicates that the ratio K/Si increases at the center of the alteration and decreases further away from it (fig. 18). The pattern is most clearly visible in the measurements from locality B where the peak of the K/Si ratio is prominent (fig. 18a). At locality C, only one of the cross-sections picked up a change in the K/Si ratio (fig. 18b). The ratio K/Si is significantly lower at locality E (0.04-0.14) than at all other localities (fig. 18d). At the other localities, the ratio generally begins at 0.1. For full data see Appendix B, table B11 to B15.

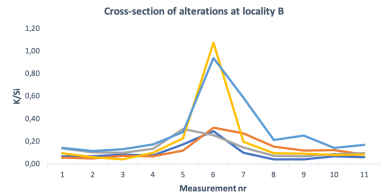

(a) Locality B

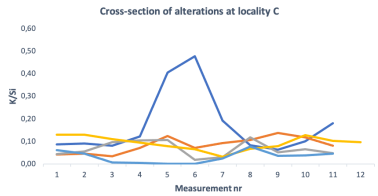

(b) Locality C

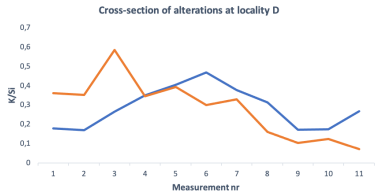

(c) Locality D

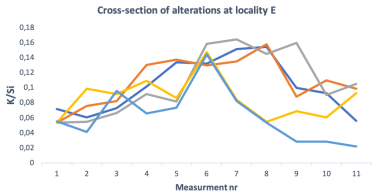

(d) Locality E

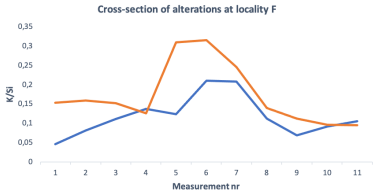

(e) Locality F

Figure 18: *Across the alterations, the ratio K/Si generally increases in the center of the cross-section and decreases towards the edges.*

5.3 Petrographic analysis

The petrographic analysis through point counting shows that the host rocks are dominated by plagioclase, hornblende and biotite, which indicates metamorphism of a mafic protolith at amphibolite conditions (table 1). All outcrops consist of more than 40% plagioclase, up to as much as 62%. The garnet-bearing localities are A, B and C. The amount of hornblende varies greatly between the localities, from 0% to 32%. Similarly, the amount of biotite varies from 0% to 32%. In addition, the amount of quartz is highly variable, from 2% to as much as 37%. However, the amount of quartz never exceeds that of plagioclase. Therefore, it is evident that the variation of modal abundance of biotite, quartz and hornblende is the main difference between the localities.

Table 1: *The point counting results is presented in the following table and the amount of minerals in the thin sections is presented in volume %. The amount of points for each mineral and the respective point counting standard error is presented in Appendix C, table C1.*

Thin section	**Volume %**						
	Plag	Hbl	Gt	Chl	Bt	Qz	Other
Host rocks							
A-1	62.2	30.0	0	3.0	0.4	2.0	2.4
A-2	57.8	32.4	0	0.4	5.8	3.6	0
A-3	57.4	32.4	0	1.8	4.4	4.0	0
B-1	57.2	7.2	2.8	4.2	0.2	14.8	13.6
B-2	50.4	9.0	0	7.0	1.0	17.6	13.0
C-1	48.0	0	10.6	1.2	31.8	8.4	0
C-2	52.0	19.4	8.6	0	15.6	4.4	0
C-3	53.8	30.6	1.8	2.8	3.0	8.0	0
C-4	45.4	2.6	12.4	0	23.4	15.2	1.0
D-1	48.2	0	0	0	13.8	37.4	0
D-2	42.8	0	0	0.6	19.4	33.0	4.2
E-1	52.0	6.0	0	0	12.6	29.2	0.2
E-2	61.6	5.6	0	0	15.2	17.6	0
F-1	57.2	9.2	0	0	17.8	15.8	0
F-2	45.4	10.4	0	0	19.6	24.2	0.2
Megacrystic garnet							
A-4a	21.4	10.8	59.6	2.2	1.4	1.4	3.2
A-4b	3.0	0.2	93.8	0.6	0	1.8	0.6

It should be noted that the modal abundances of the minerals may vary within a locality as well. For example, C-1 contains no hornblende whereas C-3 contains 30%. This implies that there is great variation within the locality. On the contrary, the other localities have a consistency in modal abundance. The column for "other" in the table represents points that could not be counted as minerals. For example, if the specific point was on a heavily altered area or if there were stains of glue on the thin section.

Chlorite mainly occurs in cracks and at rims of other crystals. It is observed that biotite has crystallised at rims of other crystals, but also occurs as individual crystals (fig. 19b). In all thin sections except those from locality A, hornblende and biotite is involved in retrograde reaction with each other (fig. 19e). In general, where hornblende is consumed, the amount of biotite increases. Furthermore, the hornblende crystals decreases in size through thin sections A to F. The opposite is observed for quartz. The size of the quartz crystals increases through thin sections A to F, and quartz shows as dynamic recrystallisation crystals in thin sections A to C whereas they occur both as large clear crystals and as smaller crystals in thin sections E to F.

The Michel-Levy analysis showed that the feldspars become increasingly anorthitic in composition from locality A to F (table 2). The percent of anorthite peaks at localities C and E. The chart used for determining the percent of anorthite in relation to the maximum extinction angle is provided in appendix A.

Table 2: *The results from the Michel-Levy analysis showed that the amount of anorthite generally increases from locality A to F. Note that the standard error is reported relative to the average, and not the extinction angle provided in the table. All of the angles measured are provided in Appendix C, table C2.*

Locality	Plag measured	Max. extinction angle	SE	% Anorthite
A	7	13.5	2.03	27
B	5	8.0	0.86	25
C	8	25	5.22	45
D	1	14	ND	30
E	7	25	3.72	45
F	5	20	2.67	36

Both the smaller garnets and the large garnets contain inclusions of plagioclase, amphibole, biotite and quartz that are quite large (fig. 19c). The smaller garnet crystals, observed in the thin sections from locality C, does not show a visible strain shadow. The garnet crystals are anhedral on a microscopic level (fig. 19a). In thin section A-4a, the strain shadow of the megacrystic garnet is observed. Closest to the garnet rim, there is no hornblende occurring and it is dominated by plagioclase and quartz. Further from the garnet rim, outside the strain shadow, hornblende and plagioclase are again dominating.

Thin section E-3 was not point counted because it is heavily altered and the crystals are very small, meaning that it was not possible to point count accurately. Also, thin section E-3 was sampled on an alteration. However, thin section E-3 is the only sample that contains epidote (fig. 19f). Epidote does not appear as single crystals, but is replacing plagioclase and hornblende. Thin sections C-6 and C-7 were also not point counted because they represent alterations. However, in thin section they appear migmatitic in texture.

The amount of microstructures identified are scarce. There are no visible inclusion trails in the garnet crystals, however the garnets are cracked in random orientations (fig. 19a). The crystals from B to F are generally flattened, indicating high pressure in one stress direction. The flattening is especially visible in thin sections from locality D, where plagioclase crystals are slightly elongated with quartz crystallised at the rims (fig. 19d).

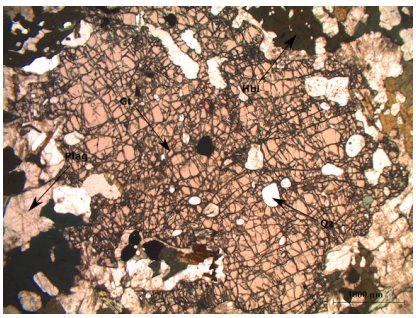

(a) The garnet rims are anhedral. Thin section C-3, PPL and 2.5x magnification.

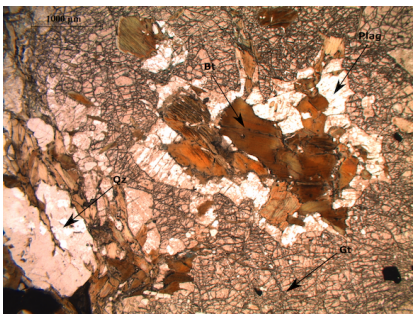

(b) Inclusion of biotite in a garnet. Thin section C-1, PPL and 2.5x magnification.

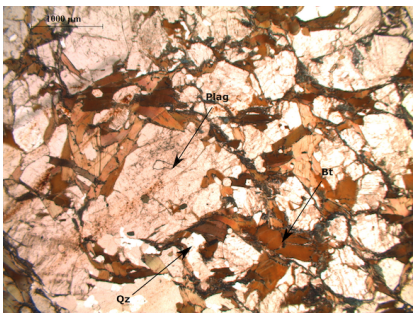

(c) Biotite has crystallised at rims of plagioclase. Thin section C-4, PPL and 2.5x magnification.

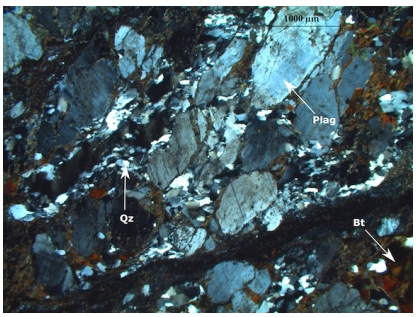

(d) Quartz crystals formed during dynamic recrystallisation. Thin section D-2, XPL and 2.5x magnification.

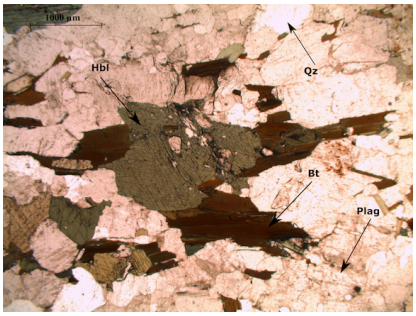

(e) A retrograde reaction between biotite and hornblende. Thin section E-2, PPL and 2.5x magnification.

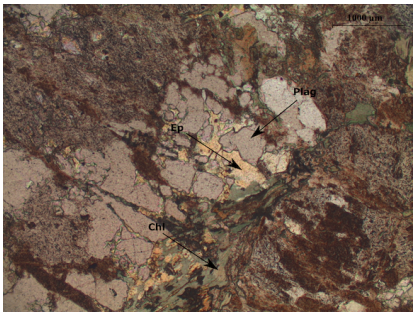

(f) A retrograde reaction between epidote and plagioclase. Thin section E-3, PPL and 2.5x magnification.

Figure 19: *The thin sections display many features.*

6 Discussion

The host rocks in this study mainly consist of hornblende, plagioclase and biotite, which is typical for amphibolite facies metamorphism of a mafic protolith. The large amount of biotite in some of the rocks could imply a pelitic protolith. However, the lack of muscovite and the abundance of hornblende makes it unlikely. Therefore, it is probable that the host rocks are mafic. The layering in the outcrop at locality A could be primary or secondary (fig. 4). The chemical analysis shows that the compositional variation is more gradational which is typical of primary, sedimentary layering. Therefore, secondary (gneissose) layering can probably be ruled out. Hence, it is most likely a pre-metamorphic layering formed by crystallisation processes in a magma chamber.

As observed in previous studies, igneous layering occurs in the most mafic, bottom part of an igneous body [Pons et al., 2006]. Layering was only found at locality A, which indicates that it was closer to the base of the magma chamber than the other localities. The chemical analysis of the Fe/Si ratio of the host rocks and the point counting results both show that localities A and C are more mafic while B, D, E and F are more felsic (cp fig. 10 and table 1). In the petrographic analysis, it is observed that the amount of quartz generally increases from locality A to B and C to F. The pattern of increasing amount of felsic minerals from the bottom to the top in an igneous intrusion has been observed in other layered intrusions, including the Skaergaard and the Muskox intrusion [Larsen and Tegner, 2006, Philpotts and Ague, 2009]. These observations could imply that localities A and C are closer to the base of the magma chamber than localities B, D, E and F. Furthermore, the repeated sequence of mafic to felsic from A to B and from C to F could indicate two injection events of magma into the chamber.

The large garnets display compositional zoning of X_{sps} and the cross-sections form a classical bell-shaped pattern as is considered typical for garnets [Ferry and Spear, 1978]. The interpretation is that the garnets grew during prograde metamorphism, where spessartine crystallized earlier due to its lower crystallisation temperature. When comparing the amount of X_{sps} in the smaller garnets at localities B and C with the large garnets at locality A, it can be observed that the large garnets have a higher value of X_{sps} in the cores (cp fig. 11 & 14). It is possible that there is no difference but that the smaller garnets were not measured precisely at the core, however it seems unlikely that such an error occurred in all 50 measurements of smaller garnets. Instead, it implies that the larger garnets initiated growth at an earlier stage than the smaller garnets and therefore suggesting two growth events of garnets. Furthermore, it is probable that the small garnets also contain compositional zoning, but that the method of measurement was not sensitive enough to notice.

It is not possible to observe any inclusion trails within the garnets nor in the matrix, which could imply that the garnets grew rapidly. Nevertheless, the garnets contain inclusions which are randomly oriented. The inclusions in the garnets indicate that the garnets grew at a later stage than the other minerals. Alternatively, there was a two-stage growth process where the other minerals, such as biotite, grew at an early stage of metamorphism but was later overgrown by garnet with increasing metamorphic grade. The anhedral crystal faces also implies lack of space during garnet growth, which further indicates growth at a later stage in the metamorphic history of the outcrops.

Spiess and Bell [1996] proposed that intensified foliation of the matrix can restrict the supply of nutrients to the growing porphyroblast which eventually leads to termination of growth. The large garnet display depletion halos which could indicate that the supply of garnet constituents ultimately limited growth. Even though the smaller garnets do not display strain shadows, the large garnets have clear and visible strain shadows in the field and in thin section. It is likely that a combination of factors contributed to termination of growth, which includes that during exhumation the rocks simply moved out of the stability field of garnet.

When comparing the results in this study with previous studies of garnet porphyroblasts, it is evident that the reason for anomalous growth is complex. In the thin sections there is no direct evidence of metamorphic fluids, such as fluid inclusions. However, a large proportion of the thin sections consists of hydrated minerals, for example biotite and hornblende, which provide indirect evidence of metamorphic fluid flow. Metamorphic fluids have previously been recognized as the main controlling factor on anomalous large garnet growth [Goldblum and Hill, 1992]. Thus, it is not unlikely that metamorphic fluids was a vital factor when the garnets in Rimbo grew.

At Gore mountain, the occurrence of large garnets were investigated and the structural geology of nearby bedrock regions were considered [Goldblum and Hill, 1992]. It was found that the relationship between two rock bodies of different evolution histories could create favourable conditions for growth of megacrystic garnets. This is a key suggestion, because it was considered that not only the microstructures in the host rock itself could provide a route for metamorphic fluids to enter the system, but also that the relationship between the host rock and adjacent rock bodies may have an effect. Furthermore, during an investigation of the garnets at Gore Mountain, it was proposed that the garnets formed due to interaction of fluids and gabbroic rocks at amphibolite facies [McLelland and Selleck, 2011]. The results of the present study does not allow for detailed analysis of possible metamorphic fluid flow. Nevertheless, the large amount of fractures and displacement in the outcrops that was found during the geological descriptions, could have

offered a route for metamorphic fluids.

The garnets formed in three out of six outcrops, and the main difference between the host rocks is the amount of mafic and felsic minerals. Therefore, it is vital to consider the influence of the bulk composition of the host rock. Formation of garnet could be favoured in mafic rocks because two of the main elements in the mineral is iron and magnesium, which mainly occur in other mafic minerals. In this study, the garnets consist of around 80% X_{alm} and only minor amounts of the other garnet species. Thus, a host rock with a large amount of mafic minerals contain the nutrients required for garnet growth. However, chemical analysis shows that localities A and C have very similar bulk composition (fig. 10). Since the large garnets only occur in locality A, it can be concluded that the bulk composition is not the cause of anomalous growth of garnets. However, as previosly mentioned, a more mafic bulk composition could have created a favourable environment for garnet growth despite not being the ultimate cause of anomalous growth.

As pointed out by Stallard [1998], porphyroblasts close in proximity may differ greatly in size and petrogenetic history, despite having formed in near-identical P-T conditions. It is likely that the garnets in Rimbo have formed in similar P-T conditions due to the short distances between the garnet-bearing outcrops. Nevertheless, the anomalous large garnets only formed in one of three outcrops. Therefore, local variation within the intrusion must be taken into consideration. In the first description of the outcrops, it was suggested that locality A might be located in a fold, which would allow metamorphic fluids to aid the growth of large garnets [Johansson et al., 2018]. Since there are no other indicators as to why the large garnets only grew at locality A, it is probable that local deformation, such as a fold, in combination with metamorphic fluids had a significant role.

Based on the chemical analysis of the alterations, it can be concluded that the change of colour is caused by an increase of potassium which possibly indicates a transition from plagioclase feldspar to K-feldspar. Additionally, the pink color of the alterations strengthens this interpretation. This suggests that the cracks were channeled by a fluid rich in K^+. Chlorite and biotite may form at the expense of hornblende during retrograde metamorphism, in the presence of K^+-rich fluids [Ahn and Cho, 1998]. Therefore, the occurrence of biotite in association with hornblende in localitites D, E and F could be interpreted as result of further hydration of hornblende. This implies that these alterations occurred after regional metamorphism and constitute a separate event in the bedrock's petrogenetic history, essentially after the formation of garnets.

The main difference between the host rocks is the grade of alteration. Localities E and F are located close to an unspecified zone of deformation which could have caused increased local alteration (fig. 2). The result of

the petrographic analysis shows that thin section E-3, which was sampled on an alteration, contains epidote. On the contrary, the chemical analysis of the alterations shows increase in potassium content but epidote does not contain potassium. However, alkali metasomatism could also bring sodium and calcium, where calcium is a constituent in epidote. Furthermore, the observed increase in anorthitic content from A to F implies a general increase in calcium. All in all, the analysis of the alterations could indicate a low-grade metamorphic overprint which is retrograde.

6.1 Source of errors and future work

There are several sources of errors related to the XRF-measurements. There was moss and lichen growing on the outcrops, meaning that some features of the host rocks may have been overlooked. Especially at locality E, the rocks were covered with mud and vegetation so it was difficult to identify the features of the outcrop. Furthermore, the methodology itself may have affected the results, for example it can be argued if the amount of measurements is enough to regard it representative of the outcrop. Finally, the samples that were collected may not be representative of the mineralogy of the outcrop. For example, locality E clearly contains epidote, which was observed during field analysis, however this was not found in the petrographic analysis. Hence, a study with a wider range of samples could improve the reliability of the results.

Further elaboration of this study could include sampling of the outcrops in order to do a laboratory-based XRF-analysis. This would allow more accurate measurements of the bulk composition of the host rock which could detect finer changes between the outcrops. Furthermore, a detailed analysis of the garnet crystals in the laboratory enables more precision in measurement of the compositional zoning. In addition, both garnet and biotite is present in the outcrops, meaning that with a microprobe analysis of their respective compositions, exact temperature conditions could be calculated using the garnet-biotite geothermometer (GARB). In turn, the garnet-Al-silicate-plagioclase geobarometer (GASP) could be used to constrain pressure conditions. This would allow the exact P-T conditions of formation of the large garnets to be calculated. Lastly, since the influence of metamorphic fluid flow is likely significant, it would be of interest to evaluate possible evidence and models of metamorphic fluid flow in the outcrops.

7 Conclusion

The aim of this study was to test the hypotheses that the outcrops represent parts of a former layered igneous intrusion and to find the reason for occurrence of large garnets. The collected data suggests that the outcrops represent a layered igneous intrusion. The chemical analysis in the field and the petrographic analysis combined presents three main confirmations of the hypothesis. Firstly, the mineral assemblages are typical for mafic rocks metamorphosed at amphibolite conditions. Secondly, the gradual change of iron and silica indicates igneous layering rather than gneissose banding. Lastly, the increase in quartz in the thin sections imply that the protoliths are increasingly felsic from A to B and C to F. It is recognized that the repeating sequence of mafic to felsic in the rocks might indicate two magma injection events.

Through previous studies of garnet porphyroblasts, the complexity of the process of formation has been recognized. In this study, it is shown that the anomalously large garnets exhibit compositional zoning, indicating prograde growth. The smaller garnets occurring in nearby outcrops have smaller amount of X_{sps} in the cores which indicates later initialisation of garnet growth at localities B and C. The lack of inclusion trails and other microstructures imply rapid growth of the garnets. The possible feldspar alteration in the host rocks likely occurred after the formation of garnets and thus had no significant effect on porphyroblast growth.

It is not evident as to why the garnets at locality A are larger than those at localities B and C. Based on the data collected in this study, a reason for occurrence of large garnets cannot be proposed. Anomalous garnet porphyroblast growth will likely continue to be a subject of intense research in the future. The understanding of the processes that govern its formation will lead to greater knowledge of various mechanisms active in bedrock during metamorphism.

References

Jung Ho Ahn and Moonsup Cho. Submicroscopic alteration of hornblende in the amphibolitic schists, northwestern Okchon metamorphic belt. *Geosciences Journal*, 2(4):165–174, December 1998. ISSN 1598-7477. doi: 10.1007/BF02910162. URL https://doi.org/10.1007/BF02910162.

Per-Gunnar Andréasson. *Geobiosfären*. Studentlitteratur AB, Lund, andra upplagan edition, 2015. ISBN 978-91-44-09639-1.

M. P. Atherton. The variation in garnet, biotite and chlorite composition in medium grade pelitic rocks from the Dalradian, Scotland, with particular reference to the zonation in garnet. *Contributions to Mineralogy and Petrology*, 18(4):347–371, August 1968. ISSN 1432-0967. doi: 10.1007/BF00399696. URL https://doi.org/10.1007/BF00399696.

T. Bell, Michael Rubenach, and P. FLEMING. Porphyroblast nucleation, growth and dissolution in regional metamorphic rocks as a function of deformation partitioning during foliation development. *Journal of Metamorphic Geology - J METAMORPH GEOL*, 4:37–67, February 1986. doi: 10.1111/j.1525-1314.1986.tb00337.x.

R. Grant Cawthorn. Layered Mafic Intrusions. In *Reference Module in Earth Systems and Environmental Sciences*. Elsevier, January 2020. ISBN 978-0-12-409548-9. doi: 10.1016/B978-0-08-102908-4.00011-4. URL http://www.sciencedirect.com/science/article/pii/B9780081029084000114.

J. M. Ferry and F. S. Spear. Experimental calibration of the partitioning of Fe and Mg between biotite and garnet. *Contributions to Mineralogy and Petrology*, 66(2):113–117, April 1978. ISSN 1432-0967. doi: 10.1007/BF00372150. URL https://doi.org/10.1007/BF00372150.

Eric C. Ferré, Stephanie M. Maes, and Kevin C. Butak. The magnetic stratification of layered mafic intrusions: Natural examples and numerical models. *Lithos*, 111(1):83–94, July 2009. ISSN 0024-4937. doi: 10.1016/j.lithos.2009.03.042. URL http://www.sciencedirect.com/science/article/pii/S0024493709001182.

Deborah R. Goldblum and Mary Louise Hill. Enhanced Fluid Flow Resulting from Competency Contrast within a Shear Zone: The Garnet Ore Zone at Gore Mountain, NY. *The Journal of Geology*, 100(6):776–782, 1992. ISSN 0022-1376. URL https://www.jstor.org/stable/30065046. Publisher: The University of Chicago Press.

Rafael F. Hartung, Luiz S. A. Simões, Rudolph A. J. Trouw, and Alex J. C. A. Silva. Growth mechanism of garnet megaporphyroblasts of the

Passos Nappe, Southern Brasília Orogen, Brazil. *Journal of South American Earth Sciences*, 102:102649, October 2020. ISSN 0895-9811. doi: 10.1016/j.jsames.2020.102649. URL http://www.sciencedirect.com/science/article/pii/S0895981120301929.

Åke Johansson, Risto Kumpulainen, and Nina Rantakokko. Sveriges största granater? *Geologiskt forum*, 2018(99):6–9, 2018.

William M. Kelly. Gore mountain's garnets. *Natural History*, 101(5):33, May 1992. ISSN 00280712. URL https://ezp.sub.su.se/login?url=http://search.ebscohost.com/login.aspx?direct=true&db=aph&AN=9205042892&site=ehost-live&scope=site. Publisher: Natural History Magazine, Inc.

Cornelis Klein and Anthony R. Philpotts. *Earth materials: Introduction to Mineralogy and Petrology*. Cambridge University Press, 2nd edition edition, 2017. ISBN 978-1-316-60885-2.

Rune B. Larsen and Christian Tegner. Pressure conditions for the solidification of the Skaergaard intrusion: Eruption of East Greenland flood basalts in less than 300,000years. *Lithos*, 92(1):181–197, November 2006. ISSN 0024-4937. doi: 10.1016/j.lithos.2006.03.032. URL http://www.sciencedirect.com/science/article/pii/S0024493706001022.

Thomas Lundqvist and Birgitta Bygghammar. Urberget. In Curt Fredén, editor, *Berg och jord*, number 12 in Sveriges Nationalatlas, pages 16–22. Sveriges Nationalatals Förlag, Kiruna, 1994. ISBN 978-91-87760-56-3.

Daniel Martin. Crystal settling and in situ crystallization in aqueous solutions and magma chambers. *Earth and Planetary Science Letters*, 96(3):336–348, January 1990. ISSN 0012-821X. doi: 10.1016/0012-821X(90)90011-L. URL http://www.sciencedirect.com/science/article/pii/0012821X9090011L.

James M. McLelland and Bruce W. Selleck. Megacrystic Gore Mountain–type garnets in the Adirondack Highlands: Age, origin, and tectonic implications. *Geosphere*, 7(5):1194–1208, October 2011. ISSN 1553-040X. doi: 10.1130/GES00683.1. URL http://pubs.geoscienceworld.org/geosphere/article/7/5/1194/132485/Megacrystic-Gore-Mountaintype-garnets-in-the.

K. Mezger, E. J. Essene, and A. N. Halliday. Closure temperatures of the Sm—Nd system in metamorphic garnets. *Earth and Planetary Science Letters*, 113(3):397–409, October 1992. ISSN 0012-821X. doi: 10.1016/0012-821X(92)90141-H. URL http://www.sciencedirect.com/science/article/pii/0012821X9290141H.

O. Namur, Bénédicte Abily, Alan E. Boudreau, Francois Blanchette, John W. M. Bush, Georges Ceuleneer, B. Charlier, Colin H. Donaldson, Jean-Clair Duchesne, M. D. Higgins, D. Morata, Troels F. D. Nielsen, B. O'Driscoll, K. N. Pang, Thomas Peacock, Carl J. Spandler, Atsushi Toramaru, and I.V. Veksler. Igneous Layering in Basaltic Magma Chambers. In Bernard Charlier, Olivier Namur, Rais Latypov, and Christian Tegner, editors, *Layered Intrusions*, Springer Geology, pages 75–152. Springer Netherlands, Dordrecht, 2015. ISBN 978-94-017-9652-1. doi: 10.1007/978-94-017-9652-1_2. URL https://doi.org/10.1007/978-94-017-9652-1_2.

Anthony R. Philpotts and Jay J. Ague. *Principles of igneous and metamorphic petrology*. Cambridge University Press, 2nd edition edition, 2009. ISBN 978-0-521-88006-0.

L. van der Plas and A. C. Tobi. A chart for judging the reliability of point counting results. *American Journal of Science*, 263(1):87–90, January 1965. ISSN 0002-9599, 1945-452X. doi: 10.2475/ajs.263.1.87. URL https://www.ajsonline.org/content/263/1/87. Publisher: American Journal of Science Section: Articles.

J. Pons, P. Barbey, H. Nachit, and J. P. Burg. Development of igneous layering during growth of pluton: The Tarçouate Laccolith (Morocco). *Tectonophysics*, 413(3):271–286, February 2006. ISSN 0040-1951. doi: 10.1016/j.tecto.2005.11.005. URL http://www.sciencedirect.com/science/article/pii/S0040195105005834.

Frank S. Spear and Frank P. Florence. Thermobarometry in granulites: pitfalls and new approaches. *Precambrian Research*, 55(1):209–241, March 1992. ISSN 0301-9268. doi: 10.1016/0301-9268(92)90025-J. URL http://www.sciencedirect.com/science/article/pii/030192689290025J.

R. Spiess and T.H. Bell. Microstructural controls on sites of metamorphic reaction: A case study of the inter-relationship between deformation and metamorphism. *European Journal of Mineralogy*, 8(1):165–186, 1996. doi: 10.1127/ejm/8/1/0165.

A. Stallard. Episodic porphyroblast growth in the Fleur de Lys Supergroup, Newfoundland: timing relative to the sequential development of multiple crenulation cleavages. *Journal of Metamorphic Geology*, 16(6):711–728, 1998. ISSN 1525-1314. doi: https://doi.org/10.1111/j.1525-1314.1998.00167.x. URL http://onlinelibrary.wiley.com/doi/abs/10.1111/j.1525-1314.1998.00167.x. _eprint: https://onlinelibrary.wiley.com/doi/pdf/10.1111/j.1525-1314.1998.00167.x.

Aaron Stallard and Ken Hickey. A comparison of microstructural and chemical patterns in garnet from the Fleur de Lys Supergroup, Newfoundland. *Journal of Structural Geology*, 24(6):1109–1123, June 2002. ISSN 0191-8141. doi: 10.1016/S0191-8141(01)00095-5. URL http://www.sciencedirect.com/science/article/pii/S0191814101000955.

R.J. Tracy, P. Robinson, and A.B. Thompson. Garnet composition and zoning in the determination of temperature and pressure of metamorphism, central Massachusetts. *American Mineralogist*, 61:762–775, 1976.

Carl-Henric Wahlgren and Kristian Schoning. Stockholmsområdets berggrund, jordarter, geologiska utveckling och erfarenheter från infrastrukturprojekt. page 108, 2018.

M.L. Williams. Sigmoidal inclusion trails, punctuated fabric development, and interactions between metamorphism and deformation. *Journal of Metamorphic Geology*, 12(1):1–21, 1994. doi: 10.1111/j.1525-1314.1994.tb00001.x.

Xiaoqi Zhang, Hongfu Zhang, and Haibo Zou. Rift-related Neoproterozoic tholeiitic layered mafic intrusions at northern Yangtze Block, South China: Mineral chemistry evidence. *Lithos*, 356-357:105376, March 2020. ISSN 0024-4937. doi: 10.1016/j.lithos.2020.105376. URL http://www.sciencedirect.com/science/article/pii/S002449372030013X.

Appendix A Michel-Levy chart

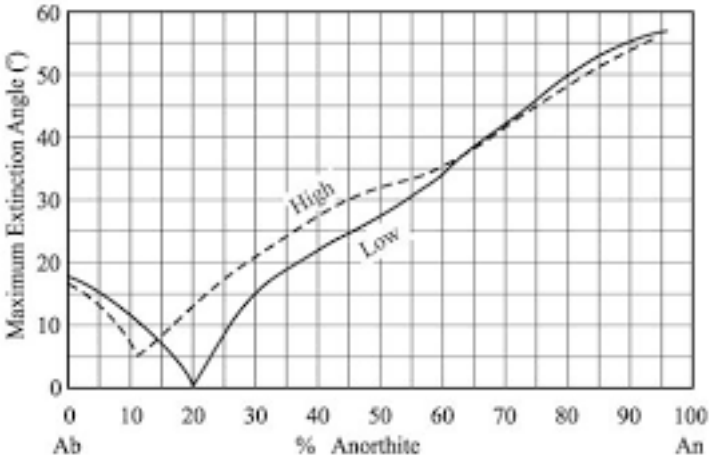

Figure A1: *The Michel-Levy chart that is used to establish the percent of anorthite of a plagioclase feldspar based on the maximum extinction angle.*

Appendix B Full data from XRF-measurements

Table B1: The table presents the data from the XRF-analysis of the host rock at locality A. The elements are given in wt.% with their respective standard error. ND is an abbreviation for "No Data".

XRF-measurements of host rock at locality A

Sample	wt.% element																	
number	Mg	Mg +/-	Al	Al +/-	Si	Si +/-	K	K +/-	Ca	Ca +/-	Ti	Ti +/-	Mn	Mn +/-	Fe	Fe +/-	LE	LE +/-
1	ND	ND	2.76	0.10	8.94	0.09	0.60	0.01	4.07	0.03	0.46	0.01	0.07	0.00	9.44	0.07	73.41	0.20
2	ND	ND	2.39	0.09	9.80	0.12	0.46	0.01	4.33	0.05	0.33	0.01	0.07	0.00	7.07	0.08	73.48	0.68
3	ND	ND	2.25	0.09	7.94	0.08	0.50	0.01	3.75	0.03	0.30	0.01	0.07	0.00	8.06	0.06	76.89	0.17
4	ND	ND	1.56	0.08	5.83	0.07	0.34	0.01	4.05	0.03	0.25	0.01	0.12	0.00	9.95	0.07	77.63	0.17
5	ND	ND	2.52	0.10	7.61	0.08	0.41	0.01	3.92	0.03	0.25	0.01	0.09	0.00	7.03	0.05	77.94	0.17
6	ND	ND	2.39	0.09	8.07	0.08	0.37	0.01	3.91	0.03	0.19	0.01	0.08	0.00	7.10	0.05	77.66	0.16
7	ND	ND	2.73	0.09	8.58	0.11	0.43	0.01	3.58	0.04	0.23	0.01	0.07	0.00	5.74	0.06	76.61	0.69
8	3.62	0.99	1.46	0.08	4.73	0.08	0.39	0.01	3.08	0.04	0.22	0.01	0.07	0.00	6.51	0.08	79.70	0.83
9	ND	ND	2.61	0.10	9.16	0.09	0.38	0.01	4.76	0.03	0.19	0.01	0.07	0.00	5.83	0.05	76.82	0.18
10	ND	ND	2.21	0.09	8.73	0.08	0.88	0.01	3.47	0.02	0.18	0.01	0.07	0.00	6.74	0.05	77.51	0.16
11	ND	ND	2.75	0.09	9.48	0.09	0.32	0.01	4.16	0.03	0.25	0.01	0.06	0.00	5.51	0.04	77.26	0.17
12	ND	ND	2.58	0.09	8.32	0.08	0.40	0.01	4.08	0.03	0.14	0.01	0.05	0.00	4.62	0.03	79.63	0.15
13	ND	ND	2.63	0.10	7.22	0.10	0.84	0.01	3.91	0.05	0.32	0.01	0.11	0.00	8.07	0.09	74.56	0.72
14	ND	ND	2.83	0.09	11.12	0.09	0.30	0.01	4.55	0.03	0.16	0.01	0.07	0.00	4.61	0.03	76.17	0.16
15	ND	ND	2.50	0.09	8.90	0.12	0.55	0.01	4.27	0.05	0.24	0.01	0.15	0.01	9.28	0.10	71.63	0.68
16	ND	ND	3.66	0.10	11.37	0.09	0.53	0.01	3.98	0.03	0.21	0.01	0.07	0.00	4.69	0.03	75.30	0.17
17	ND	ND	2.78	0.09	8.73	0.08	0.46	0.01	3.48	0.02	0.35	0.01	0.06	0.00	5.23	0.04	78.69	0.16
18	ND	ND	2.13	0.09	7.79	0.08	0.33	0.01	3.94	0.03	0.14	0.01	0.05	0.00	5.12	0.04	80.30	0.15
19	ND	ND	2.71	0.09	8.49	0.08	0.36	0.01	3.86	0.03	0.16	0.01	0.06	0.00	4.39	0.03	79.78	0.15
20	ND	ND	2.64	0.09	8.19	0.10	0.36	0.01	4.41	0.05	0.28	0.01	0.08	0.00	5.85	0.06	76.17	0.68
21	3.19	0.91	2.55	0.10	7.88	0.11	0.47	0.01	3.97	0.05	0.21	0.01	0.07	0.00	6.63	0.08	74.81	0.72
22	ND	ND	2.75	0.09	9.64	0.08	0.46	0.01	4.20	0.03	0.28	0.01	0.09	0.00	6.87	0.05	75.49	0.17
23	ND	ND	1.78	0.09	7.39	0.08	0.33	0.01	4.36	0.03	0.22	0.01	0.12	0.01	8.54	0.07	77.03	0.19
24	ND	ND	2.65	0.09	9.23	0.08	0.37	0.01	4.54	0.03	0.27	0.01	0.11	0.00	7.92	0.05	74.68	0.17
25	ND	ND	1.83	0.10	6.92	0.08	0.70	0.01	3.31	0.03	0.26	0.01	0.14	0.01	8.30	0.07	78.29	0.18

Table B2: The table presents the data from the XRF-analysis of the host rock at locality B. The elements are given in wt.% with their respective standard error.

XRF-measurements of host rock at locality B

Sample	wt.% element															
number	Al	Al +/-	Si	Si +/-	K	K +/-	Ca	Ca +/-	Ti	Ti +/-	Mn	Mn +/-	Fe	Fe +/-	LE	LE +/-
1	4.06	0.09	26.61	0.14	0.54	0.01	3.90	0.02	0.25	0.01	0.06	0.00	2.85	0.02	61.49	0.18
2	4.70	0.10	21.30	0.13	0.90	0.01	4.87	0.03	0.37	0.01	0.09	0.00	4.66	0.03	62.84	0.20
3	4.06	0.10	21.22	0.13	0.89	0.01	4.72	0.03	0.49	0.01	0.09	0.00	4.36	0.03	63.91	0.19
4	5.28	0.10	20.75	0.12	0.97	0.01	5.21	0.03	0.32	0.01	0.09	0.00	4.50	0.03	62.62	0.19
5	6.24	0.11	23.52	0.13	1.08	0.01	5.32	0.03	0.31	0.01	0.08	0.00	4.12	0.03	59.05	0.19
6	4.42	0.09	26.22	0.13	0.72	0.01	4.07	0.02	0.33	0.01	0.07	0.00	3.98	0.03	59.98	0.18
7	5.09	0.10	25.60	0.13	1.02	0.01	4.27	0.02	0.27	0.01	0.08	0.00	3.90	0.03	59.45	0.19
8	3.93	0.09	20.58	0.12	0.55	0.01	4.38	0.02	0.27	0.01	0.07	0.00	3.59	0.02	66.42	0.18
9	3.83	0.09	22.81	0.13	0.63	0.01	4.06	0.02	0.37	0.01	0.09	0.00	4.87	0.03	63.06	0.19
10	7.21	0.11	23.59	0.12	0.27	0.01	6.85	0.03	0.34	0.01	0.08	0.00	4.03	0.03	57.32	0.19
11	7.35	0.11	22.11	0.12	0.76	0.01	6.57	0.03	0.27	0.01	0.06	0.00	3.95	0.03	58.59	0.20
12	7.64	0.11	23.88	0.12	0.50	0.01	6.23	0.03	0.30	0.01	0.06	0.00	3.13	0.02	57.95	0.19
13	6.88	0.11	22.58	0.12	0.36	0.01	6.16	0.03	0.33	0.01	0.05	0.00	3.22	0.02	60.14	0.19
14	3.78	0.09	23.01	0.13	0.53	0.01	4.41	0.03	0.28	0.01	0.07	0.00	3.57	0.03	64.14	0.19
15	3.88	0.09	21.91	0.13	0.58	0.01	4.02	0.02	0.30	0.01	0.07	0.00	3.29	0.02	65.72	0.18
16	4.36	0.10	20.47	0.12	0.62	0.01	4.74	0.03	0.35	0.01	0.13	0.00	5.39	0.03	63.62	0.19
17	4.04	0.09	21.85	0.13	0.72	0.01	4.12	0.02	0.39	0.01	0.12	0.00	5.59	0.03	62.89	0.19
18	4.87	0.09	23.79	0.13	0.35	0.01	4.68	0.02	0.45	0.01	0.10	0.00	4.85	0.03	60.64	0.19
19	2.54	0.10	16.30	0.12	0.71	0.01	2.85	0.02	0.31	0.01	0.07	0.00	3.68	0.03	73.28	0.18
20	3.68	0.09	25.89	0.13	1.52	0.01	3.41	0.02	0.21	0.01	0.07	0.00	2.58	0.02	62.39	0.18
21	4.83	0.09	23.36	0.13	0.60	0.01	4.58	0.02	0.33	0.01	0.09	0.00	4.54	0.03	61.37	0.19
22	5.45	0.10	21.14	0.12	2.48	0.02	4.35	0.02	0.41	0.01	0.13	0.01	6.10	0.04	59.60	0.20
23	5.86	0.10	21.37	0.12	0.58	0.01	5.73	0.03	0.30	0.01	0.06	0.00	4.47	0.03	61.41	0.19
24	6.27	0.11	20.18	0.12	0.72	0.01	5.85	0.03	0.24	0.01	0.07	0.00	5.64	0.03	60.65	0.20
25	2.83	0.09	12.15	0.09	0.53	0.01	4.02	0.03	0.33	0.01	0.09	0.00	5.20	0.04	74.59	0.16

Table B3: The table presents the data from the XRF-analysis of the host rock at locality C. The elements are given in wt.% with their respective standard error. ND is an abbreviation for "No Data".

XRF-measurements of host rock at locality C

Sample	wt.% element																			
number	Mg	Mg +/-	Al	Al +/-	Si	Si +/-	Cl	Cl +/-	K	K +/-	Ca	Ca +/-	Ti	Ti +/-	Mn	Mn +/-	Fe	Fe +/-	LE	LE +/-
1	ND	ND	2.06	0.09	6.15	0.09	ND	ND	0.40	0.01	5.76	0.07	0.27	0.01	0.10	0.00	4.88	0.06	78.27	0.74
2	ND	ND	2.35	0.09	6.78	0.07	ND	ND	0.34	0.01	5.67	0.04	0.41	0.01	0.11	0.00	5.71	0.04	78.42	0.16
3	3.12	0.90	1.79	0.09	5.60	0.08	ND	ND	0.37	0.01	5.40	0.06	0.31	0.01	0.13	0.01	7.15	0.08	75.90	0.73
4	ND	ND	2.27	0.09	6.24	0.07	ND	ND	0.42	0.01	5.10	0.03	0.34	0.01	0.09	0.00	5.24	0.04	80.10	0.15
5	ND	ND	1.90	0.08	5.73	0.06	ND	ND	0.39	0.01	4.96	0.03	0.30	0.01	0.13	0.00	7.06	0.05	79.34	0.16
6	ND	ND	1.20	0.07	4.57	0.05	2.48	0.15	0.29	0.01	4.31	0.03	0.28	0.01	0.11	0.00	5.87	0.04	80.69	0.19
7	ND	ND	1.52	0.08	4.79	0.06	1.77	0.16	0.75	0.01	4.52	0.03	0.24	0.01	0.10	0.00	6.55	0.05	79.53	0.20
8	ND	ND	2.18	0.08	7.35	0.07	ND	ND	0.54	0.01	5.16	0.03	0.32	0.01	0.12	0.00	6.75	0.05	77.36	0.16
9	ND	ND	2.37	0.09	7.54	0.07	ND	ND	0.39	0.01	5.82	0.04	0.50	0.01	0.10	0.00	4.70	0.03	78.37	0.15
10	ND	ND	2.99	0.09	10.54	0.09	ND	ND	0.49	0.01	5.68	0.03	0.40	0.01	0.10	0.00	5.75	0.04	73.83	0.17
11	ND	ND	1.79	0.08	6.96	0.09	ND	ND	0.59	0.01	4.00	0.04	0.34	0.01	0.12	0.00	8.06	0.09	75.74	0.69
12	ND	ND	1.80	0.08	7.72	0.10	ND	ND	0.42	0.01	4.77	0.05	0.29	0.01	0.11	0.00	6.63	0.07	75.95	0.68
13	ND	ND	2.59	0.09	10.05	0.12	ND	ND	0.37	0.01	5.15	0.05	0.26	0.01	0.06	0.00	4.61	0.05	74.75	0.64
14	ND	ND	2.37	0.09	9.19	0.08	ND	ND	0.50	0.01	4.77	0.03	0.31	0.01	0.11	0.00	6.61	0.05	75.94	0.17
15	ND	ND	2.57	0.09	8.73	0.08	ND	ND	0.30	0.01	5.71	0.04	0.35	0.01	0.10	0.00	5.16	0.04	76.86	0.16
16	ND	ND	1.98	0.08	6.49	0.07	ND	ND	0.46	0.01	5.82	0.04	0.34	0.01	0.13	0.01	7.71	0.05	76.86	0.17
17	ND	ND	1.90	0.09	5.89	0.06	ND	ND	0.89	0.01	5.13	0.03	0.29	0.01	0.14	0.00	7.76	0.05	77.75	0.16
18	ND	ND	1.33	0.20	5.73	0.14	ND	ND	0.40	0.01	4.62	0.04	0.37	0.01	0.10	0.00	6.04	0.05	81.20	0.24
19	ND	ND	2.29	0.09	6.74	0.07	ND	ND	0.47	0.01	5.85	0.04	0.28	0.01	0.11	0.00	5.63	0.04	78.42	0.16
20	ND	ND	1.50	0.08	5.40	0.08	2.03	0.17	0.35	0.01	4.88	0.06	0.40	0.01	0.09	0.00	4.96	0.06	77.94	0.75
21	ND	ND	2.41	0.15	6.44	0.10	ND	ND	0.34	0.01	5.20	0.04	0.22	0.01	0.10	0.00	5.28	0.04	79.82	0.19
22	ND	ND	1.14	0.15	5.03	0.11	2.39	0.32	0.31	0.01	4.55	0.04	0.21	0.01	0.09	0.00	4.61	0.04	81.51	0.33
23	2.96	0.86	0.99	0.07	2.79	0.05	4.04	0.15	0.28	0.01	4.38	0.05	0.23	0.01	0.13	0.01	6.98	0.08	76.99	0.70
24	ND	ND	2.64	0.13	8.30	0.10	ND	ND	0.30	0.01	6.34	0.04	0.72	0.02	0.12	0.00	6.49	0.05	74.86	0.19
25	ND	ND	1.72	0.08	5.55	0.06	ND	ND	0.43	0.01	5.02	0.03	0.34	0.01	0.11	0.00	5.98	0.04	80.64	0.15

Table B4: The table presents the data from the XRF-analysis of the host rock at locality D. The elements are given in wt.% with their respective standard error. ND is an abbreviation for "No Data".

XRF-measurements of host rock at locality D

Sample	wt.% element																			
number	Mg	Mg +/-	Al	Al +/-	Si	Si +/-	Cl	Cl +/-	K	K +/-	Ca	Ca +/-	Ti	Ti +/-	Mn	Mn +/-	Fe	Fe +/-	LE	LE +/-
1	ND	ND	2.11	0.08	13.30	0.10	ND	ND	0.53	0.01	2.30	0.02	0.16	0.01	0.06	0.00	2.94	0.02	78.38	0.15
2	ND	ND	2.51	0.10	9.56	0.12	ND	ND	1.27	0.02	3.50	0.04	0.15	0.01	0.07	0.00	3.04	0.04	77.49	0.74
3	ND	ND	1.61	0.08	6.51	0.06	1.68	0.17	0.32	0.01	2.42	0.02	0.08	0.01	0.03	0.00	1.49	0.01	85.72	0.18
4	ND	ND	2.08	0.08	9.58	0.08	ND	ND	0.53	0.01	3.23	0.02	0.35	0.01	0.13	0.00	5.34	0.04	78.50	0.15
5	ND	ND	2.06	0.09	7.51	0.10	ND	ND	0.98	0.01	3.47	0.04	0.33	0.01	0.12	0.00	5.78	0.07	76.84	0.72
6	ND	ND	2.98	0.09	12.36	0.10	ND	ND	0.72	0.01	4.91	0.03	0.44	0.01	0.13	0.01	6.82	0.05	71.38	0.18
7	3.41	1.07	1.54	0.10	9.95	0.15	ND	ND	1.20	0.02	3.39	0.05	0.34	0.01	0.13	0.01	6.18	0.08	73.67	0.84
8	ND	ND	2.95	0.10	18.86	0.13	ND	ND	1.28	0.01	3.58	0.02	0.43	0.01	0.11	0.01	6.27	0.04	66.08	0.21
9	ND	ND	2.39	0.10	10.41	0.14	ND	ND	2.17	0.03	2.72	0.03	0.77	0.02	0.15	0.01	10.22	0.12	68.13	0.69
10	ND	ND	2.34	0.09	10.00	0.08	ND	ND	0.53	0.01	3.46	0.02	0.16	0.01	0.06	0.00	2.83	0.02	80.41	0.14
11	ND	ND	1.22	0.08	6.55	0.07	2.04	0.17	0.82	0.01	3.06	0.02	0.17	0.01	0.06	0.00	2.96	0.02	82.92	0.19
12	ND	ND	4.32	0.10	19.23	0.12	ND	ND	2.34	0.02	3.45	0.02	0.47	0.01	0.15	0.01	6.87	0.04	62.79	0.20
13	ND	ND	1.07	0.07	6.92	0.07	2.44	0.17	0.42	0.01	1.61	0.01	0.13	0.01	0.07	0.00	2.89	0.02	84.26	0.19
14	ND	ND	2.94	0.09	17.92	0.11	ND	ND	1.53	0.01	2.93	0.02	0.17	0.01	0.04	0.00	1.80	0.02	72.47	0.16
15	ND	ND	2.06	0.09	11.99	0.09	ND	ND	1.99	0.01	1.62	0.01	0.21	0.01	0.08	0.00	3.55	0.03	78.30	0.15
16	ND	ND	2.27	0.09	13.48	0.11	ND	ND	0.90	0.01	2.95	0.02	0.39	0.01	0.10	0.00	4.94	0.04	74.70	0.18
17	ND	ND	2.63	0.10	15.20	0.12	ND	ND	1.18	0.01	3.25	0.02	0.32	0.01	0.10	0.00	4.66	0.04	72.34	0.19
18	ND	ND	2.50	0.09	13.05	0.10	ND	ND	1.09	0.01	4.66	0.03	0.29	0.01	0.12	0.00	6.65	0.04	71.39	0.18
19	ND	ND	3.89	0.09	23.41	0.14	ND	ND	0.62	0.01	4.65	0.03	0.27	0.01	0.07	0.00	3.74	0.03	63.13	0.19
20	ND	ND	4.51	0.10	20.61	0.13	ND	ND	0.59	0.01	4.33	0.03	0.36	0.01	0.10	0.00	5.11	0.04	64.12	0.21
21	ND	ND	2.23	0.08	11.75	0.09	ND	ND	0.52	0.01	2.10	0.01	0.13	0.01	0.04	0.00	2.19	0.02	80.84	0.13
22	ND	ND	2.44	0.10	12.11	0.10	ND	ND	0.52	0.01	2.63	0.02	0.15	0.01	0.03	0.00	1.43	0.01	80.48	0.15
23	ND	ND	2.12	0.08	13.11	0.10	ND	ND	0.61	0.01	2.27	0.02	0.19	0.01	0.07	0.00	3.36	0.02	78.05	0.15
24	ND	ND	6.72	0.11	20.53	0.12	ND	ND	0.40	0.01	5.52	0.03	0.23	0.01	0.07	0.00	3.51	0.02	62.70	0.19
25	ND	ND	3.99	0.10	22.14	0.13	ND	ND	0.95	0.01	3.28	0.02	0.32	0.01	0.09	0.00	4.64	0.03	64.31	0.20

Table B5: The table presents the data from the XRF-analysis of the host rock at locality E. The elements are given in wt.% with their respective standard error.

XRF-measurements of host rock at locality E

Sample	wt.% element															
number	Al	Al +/-	Si	Si +/-	K	K +/-	Ca	Ca +/-	Ti	Ti +/-	Mn	Mn +/-	Fe	Fe +/-	LE	LE +/-
1	2.39	0.09	14.50	0.10	0.62	0.01	3.38	0.02	0.19	0.01	0.04	0.00	2.27	0.02	76.43	0.15
2	2.91	0.09	14.79	0.10	0.72	0.01	3.91	0.02	0.22	0.01	0.05	0.00	2.88	0.02	74.33	0.16
3	2.84	0.09	14.33	0.11	0.99	0.01	3.85	0.02	0.37	0.01	0.10	0.00	6.13	0.04	71.06	0.18
4	2.36	0.09	14.23	0.11	0.78	0.01	3.27	0.02	0.30	0.01	0.06	0.00	3.91	0.03	74.87	0.16
5	3.40	0.08	27.89	0.14	0.69	0.01	3.02	0.02	0.22	0.01	0.06	0.00	3.32	0.02	61.21	0.18
6	2.94	0.09	16.04	0.11	0.60	0.01	3.52	0.02	0.25	0.01	0.05	0.00	3.32	0.02	73.08	0.16
7	4.72	0.09	25.78	0.13	0.98	0.01	4.09	0.02	0.23	0.01	0.05	0.00	2.98	0.02	60.92	0.18
8	3.04	0.09	17.57	0.11	0.78	0.01	3.57	0.02	0.23	0.01	0.05	0.00	2.90	0.02	71.69	0.16
9	1.36	0.08	10.02	0.09	0.63	0.01	2.88	0.02	0.23	0.01	0.06	0.00	3.21	0.02	81.41	0.14
10	3.17	0.09	20.03	0.11	0.52	0.01	3.81	0.02	0.11	0.01	0.03	0.00	1.18	0.01	70.99	0.16
11	2.30	0.09	13.55	0.14	0.58	0.01	3.77	0.04	0.21	0.01	0.07	0.00	3.45	0.04	73.56	0.61
12	4.21	0.09	24.79	0.13	0.82	0.01	3.68	0.02	0.25	0.01	0.06	0.00	3.09	0.02	62.90	0.18
13	2.04	0.08	8.40	0.08	0.67	0.01	3.49	0.02	0.31	0.01	0.10	0.00	5.73	0.04	79.01	0.15
14	1.89	0.08	13.52	0.10	0.45	0.01	2.86	0.02	0.15	0.01	0.04	0.00	1.79	0.02	79.13	0.14
15	2.48	0.09	14.09	0.16	0.63	0.01	3.51	0.04	0.19	0.01	0.05	0.00	2.99	0.03	73.53	0.66
16	3.48	0.10	15.49	0.11	0.68	0.01	3.95	0.02	0.22	0.01	0.05	0.00	2.82	0.02	73.11	0.17
17	3.27	0.10	13.77	0.10	0.71	0.01	3.73	0.02	0.22	0.01	0.05	0.00	2.70	0.02	75.29	0.16
18	2.05	0.09	10.60	0.09	0.85	0.01	3.07	0.02	0.40	0.01	0.09	0.00	5.77	0.04	76.94	0.17
19	3.29	0.09	18.59	0.12	0.54	0.01	4.13	0.02	0.13	0.01	0.04	0.00	1.86	0.02	71.22	0.17
20	2.19	0.09	14.15	0.10	0.49	0.01	3.54	0.02	0.14	0.01	0.03	0.00	1.56	0.01	77.73	0.15
21	1.69	0.09	12.00	0.10	0.50	0.01	3.27	0.02	0.22	0.01	0.07	0.00	2.51	0.02	79.58	0.15
22	2.25	0.09	12.84	0.10	0.63	0.01	3.63	0.02	0.17	0.01	0.05	0.00	2.03	0.02	78.23	0.15
23	2.61	0.09	14.03	0.10	0.59	0.01	4.17	0.03	0.22	0.01	0.07	0.00	3.11	0.02	74.97	0.16
24	2.18	0.09	13.30	0.10	0.64	0.01	3.92	0.02	0.18	0.01	0.05	0.00	2.65	0.02	76.87	0.15
25	5.92	0.11	21.86	0.13	0.57	0.01	5.72	0.03	0.25	0.01	0.06	0.00	3.29	0.02	62.10	0.19

Table B6: The table presents the data from the XRF-analysis of the host rock at locality F. The elements are given in wt.% with their respective standard error. ND is an abbreviation for "No Data".

XRF-measurements of host rock at locality F

Sample	wt.% element																	
number	Al	Al +/-	Si	Si +/-	Cl	Cl +/-	K	K +/-	Ca	Ca +/-	Ti	Ti +/-	Mn	Mn +/-	Fe	Fe +/-	LE	LE +/-
1	2.34	0.09	8.43	0.08	ND	ND	0.59	0.01	3.17	0.02	0.23	0.01	0.05	0.00	2.58	0.02	82.43	0.14
2	2.80	0.09	13.60	0.10	ND	ND	0.49	0.01	3.77	0.02	0.28	0.01	0.10	0.00	4.65	0.03	74.09	0.16
3	0.64	0.07	3.70	0.05	4.43	0.16	0.32	0.01	2.67	0.02	0.05	0.00	0.02	0.00	0.62	0.01	87.40	0.17
4	1.17	0.08	8.04	0.11	1.94	0.18	0.58	0.01	2.20	0.03	0.23	0.00	0.06	0.00	3.62	0.05	79.80	0.84
5	1.91	0.09	12.00	0.09	ND	ND	0.54	0.01	2.49	0.02	0.13	0.00	0.04	0.00	2.13	0.02	80.57	0.14
6	3.57	0.09	20.30	0.12	ND	ND	0.74	0.01	3.85	0.02	0.25	0.01	0.06	0.00	3.01	0.02	67.92	0.17
7	2.45	0.08	18.16	0.12	ND	ND	0.61	0.01	2.93	0.02	0.31	0.01	0.09	0.00	4.36	0.03	70.74	0.17
8	4.33	0.10	18.54	0.11	ND	ND	0.85	0.01	4.34	0.02	0.16	0.01	0.05	0.00	2.40	0.02	69.10	0.17
9	3.34	0.09	22.93	0.13	ND	ND	0.50	0.01	3.20	0.02	0.15	0.00	0.03	0.00	1.31	0.01	68.39	0.16
10	1.86	0.09	7.90	0.08	ND	ND	0.58	0.01	2.83	0.02	0.19	0.01	0.05	0.00	2.84	0.02	83.56	0.14
11	3.91	0.09	18.37	0.11	ND	ND	0.96	0.01	4.08	0.02	0.34	0.01	0.07	0.00	4.00	0.03	68.00	0.18
12	3.33	0.09	18.47	0.12	ND	ND	0.70	0.01	3.60	0.02	0.25	0.01	0.05	0.00	2.83	0.02	70.60	0.17
13	4.63	0.09	22.34	0.12	ND	ND	0.69	0.01	4.53	0.02	0.18	0.01	0.04	0.00	1.64	0.01	65.79	0.17
14	3.76	0.09	21.21	0.12	ND	ND	0.76	0.01	3.41	0.02	0.38	0.01	0.08	0.00	4.22	0.03	65.90	0.18
15	4.11	0.09	24.44	0.13	ND	ND	0.54	0.01	3.95	0.02	0.21	0.01	0.05	0.00	2.52	0.02	63.97	0.18
16	3.03	0.09	18.01	0.11	ND	ND	1.00	0.01	2.63	0.02	0.29	0.01	0.07	0.00	4.38	0.03	70.27	0.17
17	4.78	0.10	19.24	0.12	ND	ND	0.99	0.01	4.81	0.03	0.34	0.01	0.08	0.00	4.26	0.03	65.29	0.18
18	4.82	0.10	20.35	0.12	ND	ND	0.53	0.01	4.87	0.03	0.19	0.01	0.05	0.00	1.95	0.02	67.07	0.17
19	4.16	0.10	20.11	0.12	ND	ND	1.01	0.01	3.94	0.02	0.32	0.01	0.06	0.00	3.48	0.02	66.66	0.18
20	3.03	0.11	18.02	0.13	ND	ND	1.00	0.01	3.68	0.03	0.24	0.01	0.06	0.00	2.82	0.02	70.89	0.20
21	0.48	0.06	2.65	0.04	5.09	0.14	0.42	0.01	2.17	0.02	0.20	0.00	0.05	0.00	3.02	0.02	85.74	0.16
22	2.47	0.09	11.96	0.09	ND	ND	0.55	0.01	2.80	0.02	0.15	0.00	0.04	0.00	2.24	0.02	79.61	0.14
23	0.46	0.06	3.26	0.04	5.15	0.13	0.81	0.01	2.58	0.02	0.30	0.01	0.10	0.00	5.27	0.04	81.85	0.16
24	1.24	0.08	9.84	0.08	ND	ND	0.53	0.01	2.26	0.02	0.18	0.00	0.04	0.00	2.09	0.02	83.61	0.13
25	3.01	0.09	11.02	0.09	ND	ND	0.52	0.01	4.26	0.03	0.17	0.01	0.06	0.00	2.77	0.02	78.01	0.15

Table B7: The table presents the data from the XRF-analysis of the garnets at locality B. The elements are given in wt.% with their respective standard error. ND is an abbreviation for "No Data".

Measurement of garnets at locality B

Sample	wt.% element																			
number	Mg	Mg +/-	Al	Al +/-	Si	Si +/-	Cl	Cl +/-	K	K +/-	Ca	Ca +/-	Ti	Ti +/-	Mn	Mn +/-	Fe	Fe +/-	LE	LE +/-
1	ND	ND	1.50	0.14	3.38	0.08	ND	ND	0.30	0.01	3.64	0.03	0.18	0.01	1.34	0.02	15.13	0.12	74.41	0.22
2	ND	ND	0.81	0.09	1.79	0.04	4.79	0.19	0.50	0.01	2.70	0.02	0.34	0.01	1.01	0.01	14.91	0.11	72.99	0.25
3	ND	ND	1.30	0.08	3.98	0.06	2.60	0.15	0.75	0.01	3.79	0.04	0.58	0.01	0.62	0.01	15.09	0.17	69.07	0.64
4	ND	ND	1.06	0.07	2.55	0.04	3.55	0.15	0.19	0.01	3.67	0.03	0.25	0.01	1.18	0.02	17.41	0.13	70.04	0.25
5	ND	ND	0.81	0.07	1.74	0.04	4.84	0.15	0.45	0.01	2.94	0.04	0.23	0.01	1.14	0.02	17.43	0.21	67.98	0.67
6	ND	ND	1.15	0.07	2.34	0.04	2.80	0.15	0.51	0.01	3.12	0.04	0.27	0.01	1.18	0.02	15.43	0.18	71.07	0.67
7	ND	ND	1.17	0.07	2.92	0.04	2.80	0.15	0.51	0.01	3.34	0.03	0.28	0.01	1.44	0.02	18.40	0.14	69.06	0.25
8	ND	ND	1.26	0.08	2.94	0.05	3.82	0.16	0.91	0.01	3.39	0.04	0.30	0.01	0.99	0.02	15.60	0.18	68.23	0.65
9	ND	ND	1.13	0.07	3.05	0.04	4.16	0.14	0.54	0.01	3.85	0.03	0.17	0.01	1.07	0.01	15.61	0.11	70.26	0.23
10	ND	ND	0.78	0.07	2.01	0.04	4.09	0.14	0.36	0.01	2.77	0.02	0.17	0.01	1.11	0.01	16.94	0.13	71.64	0.24
11	ND	ND	1.47	0.08	3.56	0.05	2.23	0.15	0.78	0.01	3.64	0.03	0.35	0.01	0.55	0.01	9.86	0.07	77.32	0.2
12	ND	ND	1.14	0.07	2.47	0.04	3.53	0.14	0.19	0.01	3.39	0.03	0.22	0.01	1.22	0.02	16.43	0.12	71.30	0.24
13	ND	ND	0.91	0.07	2.87	0.04	3.62	0.15	0.77	0.01	2.51	0.02	0.22	0.01	1.10	0.01	16.89	0.13	70.95	0.24
14	ND	ND	1.49	0.08	3.20	0.06	1.22	0.16	0.20	0.01	3.47	0.04	0.20	0.01	1.31	0.02	18.85	0.22	67.79	0.66
15	ND	ND	0.78	0.07	1.89	0.03	5.17	0.14	0.67	0.01	2.74	0.02	0.25	0.01	0.71	0.01	15.41	0.12	72.19	0.23
16	ND	0.87	0.90	0.07	2.01	0.04	4.38	0.15	0.30	0.01	3.57	0.04	0.10	0.01	1.10	0.02	14.71	0.17	69.30	0.67
17	ND	ND	0.75	0.06	1.44	0.03	4.48	0.14	0.23	0.01	2.82	0.03	0.42	0.01	1.24	0.02	16.27	0.19	70.26	0.66
18	ND	ND	0.63	0.06	1.17	0.03	5.05	0.14	0.20	0.01	2.51	0.02	0.18	0.01	1.15	0.02	15.44	0.12	73.53	0.23
19	5.23	0.90	0.65	0.06	1.57	0.04	4.76	0.15	0.20	0.01	2.86	0.04	0.23	0.01	1.28	0.02	18.49	0.22	64.59	0.66
20	ND	ND	0.71	0.07	1.60	0.04	4.49	0.15	0.41	0.01	2.79	0.03	0.32	0.01	1.24	0.02	16.74	0.20	69.53	0.69
21	3.15	0.84	1.22	0.07	2.75	0.05	3.30	0.15	0.16	0.01	3.34	0.04	0.27	0.01	1.18	0.02	17.58	0.20	66.94	0.63
22	3.15	0.93	0.73	0.07	1.34	0.03	3.86	0.15	0.19	0.01	2.73	0.03	0.20	0.01	1.17	0.02	17.97	0.22	68.58	0.7
23	3.31	0.87	0.53	0.06	1.28	0.03	4.86	0.14	0.18	0.01	2.34	0.03	0.22	0.01	0.76	0.01	11.68	0.13	74.71	0.7
24	ND	ND	0.53	0.05	1.71	0.03	4.97	0.13	0.27	0.01	2.98	0.03	0.17	0.01	0.33	0.01	7.15	0.08	79.48	0.65
25	ND	ND	1.00	0.07	2.16	0.04	4.00	0.14	0.45	0.01	2.88	0.03	0.27	0.01	1.04	0.02	12.94	0.14	72.92	0.64

Table B8: The table presents the data from the XRF-analysis of the garnets at locality C. The elements are given in wt.% with their respective standard error. ND is an abbreviation for "No Data".

Measurement of garnets at locality C

Sample	wt.% element																			
number	Mg	Mg +/-	Al	Al +/-	Si	Si +/-	Cl	Cl +/-	K	K +/-	Ca	Ca +/-	Ti	Ti +/-	Mn	Mn +/-	Fe	Fe +/-	LE	LE +/-
1	ND	ND	1.50	0.14	3.38	0.08	ND	ND	0.30	0.01	3.64	0.03	0.18	0.01	1.34	0.02	15.13	0.12	74.41	0.22
2	ND	ND	0.81	0.09	1.79	0.04	4.79	0.19	0.50	0.01	2.70	0.02	0.34	0.01	1.01	0.01	14.91	0.11	72.99	0.25
3	ND	ND	1.30	0.08	3.98	0.06	2.60	0.15	0.75	0.01	3.79	0.04	0.58	0.01	0.62	0.01	15.09	0.17	69.07	0.64
4	ND	ND	1.06	0.07	2.55	0.04	3.55	0.15	0.19	0.01	3.67	0.03	0.25	0.01	1.18	0.02	17.41	0.13	70.04	0.25
5	ND	ND	0.81	0.07	1.74	0.04	4.84	0.15	0.45	0.01	2.94	0.04	0.23	0.01	1.14	0.02	17.43	0.21	67.98	0.67
6	ND	ND	1.15	0.07	2.34	0.04	2.80	0.15	0.51	0.01	3.12	0.04	0.27	0.01	1.18	0.02	15.43	0.18	71.07	0.67
7	ND	ND	1.17	0.07	2.92	0.04	2.80	0.15	0.51	0.01	3.34	0.03	0.28	0.01	1.44	0.02	18.40	0.14	69.06	0.25
8	ND	ND	1.26	0.08	2.94	0.05	3.82	0.16	0.91	0.01	3.39	0.04	0.30	0.01	0.99	0.02	15.60	0.18	68.23	0.65
9	ND	ND	1.13	0.07	3.05	0.04	4.16	0.14	0.54	0.01	3.85	0.03	0.17	0.01	1.07	0.01	15.61	0.11	70.26	0.23
10	ND	ND	0.78	0.07	2.01	0.04	4.09	0.14	0.36	0.01	2.77	0.02	0.17	0.01	1.11	0.01	16.94	0.13	71.64	0.24
11	ND	ND	1.47	0.08	3.56	0.05	2.23	0.15	0.78	0.01	3.64	0.03	0.35	0.01	0.55	0.01	9.86	0.07	77.32	0.2
12	ND	ND	1.14	0.07	2.47	0.04	3.53	0.14	0.19	0.01	3.39	0.03	0.22	0.01	1.22	0.02	16.43	0.12	71.30	0.24
13	ND	ND	0.91	0.07	2.87	0.04	3.62	0.15	0.77	0.01	2.51	0.02	0.22	0.01	1.10	0.01	16.89	0.13	70.95	0.24
14	ND	ND	1.49	0.08	3.20	0.06	1.22	0.16	0.20	0.01	3.47	0.04	0.20	0.01	1.31	0.02	18.85	0.22	67.79	0.66
15	ND	ND	0.78	0.07	1.89	0.03	5.17	0.14	0.67	0.01	2.74	0.02	0.25	0.01	0.71	0.01	15.41	0.12	72.19	0.23
16	ND	0.87	0.90	0.07	2.01	0.04	4.38	0.15	0.30	0.01	3.57	0.04	0.10	0.01	1.10	0.02	14.71	0.17	69.30	0.67
17	ND	ND	0.75	0.06	1.44	0.03	4.48	0.14	0.23	0.01	2.82	0.03	0.42	0.01	1.24	0.02	16.27	0.19	70.26	0.66
18	ND	ND	0.63	0.06	1.17	0.03	5.05	0.14	0.20	0.01	2.51	0.02	0.18	0.01	1.15	0.02	15.44	0.12	73.53	0.23
19	5.23	0.90	0.65	0.06	1.57	0.04	4.76	0.15	0.20	0.01	2.86	0.04	0.23	0.01	1.28	0.02	18.49	0.22	64.59	0.66
20	ND	ND	0.71	0.07	1.60	0.04	4.49	0.15	0.41	0.01	2.79	0.03	0.32	0.01	1.24	0.02	16.74	0.20	69.53	0.69
21	3.15	0.84	1.22	0.07	2.75	0.05	3.30	0.15	0.16	0.01	3.34	0.04	0.27	0.01	1.18	0.02	17.58	0.20	66.94	0.63
22	3.15	0.93	0.73	0.07	1.34	0.03	3.86	0.15	0.19	0.01	2.73	0.03	0.20	0.01	1.17	0.02	17.97	0.22	68.58	0.7
23	3.31	0.87	0.53	0.06	1.28	0.03	4.86	0.14	0.18	0.01	2.34	0.03	0.22	0.01	0.76	0.01	11.68	0.13	74.71	0.7
24	ND	ND	0.53	0.05	1.71	0.03	4.97	0.13	0.27	0.01	2.98	0.03	0.17	0.01	0.33	0.01	7.15	0.08	79.48	0.65
25	ND	ND	1.00	0.07	2.16	0.04	4.00	0.14	0.45	0.01	2.88	0.03	0.27	0.01	1.04	0.02	12.94	0.14	72.92	0.64

Table B9: The table presents the data of the cross-sections from the XRF-analysis of the anomalously large garnets at locality A. All of the garnets have different amount of measurements due to the variation in diameter. The elements are given in wt.% with their respective standard error. ND is an abbreviation for "No Data".

XRF-measurements of large garnets

Garnet	wt.% element																			
number	Mg	Mg +/-	Al	Al +/-	Si	Si +/-	Cl	Cl +/-	K	K +/-	Ca	Ca +/-	Ti	Ti +/-	Mn	Mn +/-	Fe	Fe +/-	LE	LE +/-
1	ND	ND	2.20	0.10	7.01	0.10	ND	ND	0.94	0.01	2.73	0.03	0.15	0.01	0.78	0.01	14.92	0.18	68.29	0.73
1	3.14	0.97	2.71	0.10	7.37	0.11	ND	ND	0.70	0.01	3.03	0.04	0.14	0.01	1.42	0.02	17.31	0.21	63.99	0.69
1	ND	ND	1.60	0.09	4.77	0.08	2.07	0.17	0.59	0.01	2.48	0.03	0.12	0.01	1.61	0.02	17.55	0.22	66.24	0.71
1	ND	ND	2.59	0.10	6.88	0.10	ND	ND	0.78	0.01	3.00	0.04	0.17	0.01	1.38	0.02	16.81	0.20	65.68	0.68
1	ND	ND	2.43	0.10	6.35	0.10	ND	ND	0.42	0.01	2.64	0.03	0.19	0.01	1.82	0.03	18.94	0.23	64.27	0.70
1	ND	ND	2.51	0.10	7.11	0.08	ND	ND	0.41	0.01	3.13	0.02	0.11	0.01	2.11	0.02	21.41	0.15	63.00	0.26
1	3.05	0.97	2.11	0.09	5.85	0.09	ND	ND	0.40	0.01	3.02	0.04	0.32	0.01	1.71	0.03	20.71	0.25	62.53	0.68
1	ND	ND	2.40	0.10	6.74	0.10	ND	ND	0.42	0.01	3.44	0.04	0.75	0.02	1.56	0.02	22.48	0.27	59.20	0.65
2	3.46	1.09	2.20	0.10	4.64	0.08	ND	ND	0.37	0.01	3.12	0.04	0.13	0.01	1.30	0.02	20.59	0.28	63.95	0.77
2	ND	ND	2.27	0.10	5.15	0.08	ND	ND	0.30	0.01	3.04	0.04	0.18	0.01	1.69	0.03	20.88	0.26	64.26	0.70
2	ND	ND	1.59	0.08	3.70	0.05	1.93	0.16	0.28	0.01	2.41	0.02	0.16	0.01	1.63	0.02	17.79	0.13	70.32	0.25
2	ND	ND	1.53	0.08	3.46	0.05	2.00	0.15	0.24	0.01	2.28	0.02	0.18	0.01	1.61	0.02	18.75	0.14	69.76	0.25
2	ND	ND	2.16	0.09	4.57	0.07	1.32	0.17	0.24	0.01	2.58	0.03	0.10	0.01	1.74	0.03	19.36	0.23	65.52	0.68
2	ND	ND	1.55	0.08	3.48	0.05	2.47	0.16	0.20	0.01	2.44	0.02	0.10	0.01	1.41	0.02	16.96	0.13	71.20	0.25
2	ND	ND	1.48	0.08	3.74	0.05	2.73	0.17	0.28	0.01	2.48	0.02	0.13	0.01	1.71	0.02	18.87	0.15	68.47	0.27
2	ND	ND	1.63	0.09	3.62	0.06	1.67	0.17	0.19	0.01	2.68	0.04	0.17	0.01	1.75	0.03	20.85	0.27	64.66	0.72
2	ND	ND	1.24	0.08	2.74	0.06	2.29	0.17	0.24	0.01	2.40	0.03	0.11	0.01	1.52	0.03	19.82	0.27	66.70	0.80
2	ND	ND	2.00	0.09	3.77	0.06	2.21	0.16	0.22	0.01	2.83	0.03	0.11	0.01	1.38	0.02	21.73	0.25	63.29	0.64
3	ND	ND	2.20	0.09	4.83	0.06	4.20	0.17	0.27	0.01	2.73	0.02	0.09	0.01	1.38	0.02	18.77	0.14	65.38	0.27

Continuation of table B9

	Mg	Mg +/-	Al	Al +/-	Si	Si +/-	Cl	Cl +/-	K	K +/-	Ca	Ca +/-	Ti	Ti +/-	Mn	Mn +/-	Fe	Fe +/-	LE	LE +/-
3	ND	ND	1.92	0.08	4.38	0.06	4.61	0.17	0.19	0.01	2.60	0.02	0.17	0.01	1.65	0.02	17.99	0.13	66.34	0.27
3	ND	ND	2.08	0.09	5.01	0.07	7.11	0.18	0.57	0.01	3.02	0.04	0.12	0.01	1.80	0.03	20.26	0.23	57.48	0.59
3	ND	ND	1.10	0.07	2.99	0.04	4.20	0.15	0.58	0.01	2.50	0.02	0.09	0.01	1.35	0.02	18.10	0.13	68.97	0.25
3	ND	ND	2.32	0.09	5.81	0.09	1.92	0.18	0.43	0.01	2.94	0.04	0.18	0.01	1.40	0.02	20.54	0.24	62.20	0.65
4	8.36	2.13	1.77	0.16	6.12	0.18	ND	ND	0.24	0.01	3.76	0.10	0.11	0.01	1.13	0.04	19.02	0.49	59.40	1.45
4	9.53	2.68	1.55	0.19	4.08	0.16	ND	ND	0.32	0.02	3.40	0.11	0.07	0.01	1.40	0.05	19.91	0.64	59.64	1.83
4	7.50	1.75	1.42	0.13	4.17	0.11	ND	ND	0.19	0.01	2.82	0.06	0.12	0.01	1.83	0.04	19.82	0.42	62.03	1.23
4	ND	ND	1.55	0.13	4.26	0.11	ND	ND	0.12	0.01	2.77	0.06	0.10	0.01	1.83	0.04	19.00	0.41	65.19	1.29
4	7.37	1.56	1.94	0.13	5.68	0.13	ND	ND	0.08	0.01	3.55	0.07	0.16	0.01	1.82	0.04	20.58	0.39	58.65	1.05
4	ND	ND	2.00	0.12	4.93	0.11	ND	ND	0.11	0.01	3.07	0.06	0.13	0.01	1.58	0.03	20.33	0.37	63.50	1.06
4	ND	ND	1.58	0.13	6.01	0.10	ND	ND	0.18	0.01	3.15	0.04	0.09	0.01	1.06	0.02	18.34	0.20	69.48	0.34
5	ND	ND	4.09	0.11	9.45	0.09	ND	ND	0.21	0.01	3.59	0.03	0.27	0.01	1.38	0.02	23.40	0.16	57.37	0.29
5	ND	ND	4.16	0.11	10.67	0.10	ND	ND	0.22	0.01	3.77	0.03	0.16	0.01	1.54	0.02	21.22	0.14	57.87	0.28
5	ND	ND	4.52	0.11	10.66	0.09	ND	ND	0.21	0.01	3.71	0.03	0.21	0.01	1.86	0.02	23.00	0.15	55.47	0.28
5	ND	ND	4.05	0.11	10.46	0.09	ND	ND	0.66	0.01	3.48	0.02	0.24	0.01	2.12	0.02	21.96	0.14	56.74	0.27
5	ND	ND	4.07	0.11	10.05	0.09	ND	ND	0.72	0.01	3.14	0.02	0.21	0.01	2.22	0.02	21.98	0.14	57.31	0.28
5	ND	ND	4.09	0.11	9.70	0.09	ND	ND	0.33	0.01	3.61	0.03	0.25	0.01	2.21	0.02	22.57	0.15	56.89	0.28
5	ND	ND	2.29	0.11	6.75	0.09	ND	ND	0.25	0.01	3.12	0.03	0.10	0.01	1.81	0.02	20.45	0.18	64.94	0.31
5	ND	ND	3.33	0.12	8.41	0.13	ND	ND	0.28	0.01	3.53	0.05	0.16	0.01	1.69	0.03	22.64	0.29	57.32	0.67
5	ND	ND	3.35	0.11	7.98	0.09	ND	ND	0.25	0.01	3.28	0.03	0.15	0.01	1.39	0.02	22.18	0.16	61.17	0.28
6	ND	ND	1.33	0.08	2.92	0.04	2.52	0.15	0.54	0.01	2.47	0.02	0.08	0.01	1.22	0.02	16.13	0.12	72.60	0.23
6	ND	ND	1.24	0.08	2.51	0.04	2.15	0.16	0.41	0.01	2.44	0.02	0.09	0.01	1.70	0.02	18.96	0.15	70.31	0.26
6	ND	ND	0.99	0.08	2.44	0.05	3.22	0.16	0.41	0.01	2.55	0.03	0.10	0.01	1.78	0.03	18.73	0.24	67.06	0.74
6	3.14	1.02	0.97	0.08	2.35	0.05	2.41	0.16	0.38	0.01	2.40	0.03	0.12	0.01	1.92	0.03	19.03	0.25	67.09	0.75

Continuation of table B9

	Mg	Mg +/-	Al	Al +/-	Si	Si +/-	Cl	Cl +/-	K	K +/-	Ca	Ca +/-	Ti	Ti +/-	Mn	Mn +/-	Fe	Fe +/-	LE	LE +/-
6	3.91	1.07	0.98	0.08	2.00	0.05	3.19	0.17	0.39	0.01	2.26	0.03	0.10	0.01	1.91	0.03	18.44	0.25	66.61	0.80
6	ND	ND	0.89	0.08	1.89	0.04	3.04	0.17	0.33	0.01	2.39	0.03	0.11	0.01	2.02	0.03	19.17	0.25	67.10	0.77
6	3.38	1.09	0.92	0.08	1.99	0.05	3.36	0.18	0.37	0.01	2.58	0.04	0.09	0.01	1.85	0.03	18.44	0.26	66.86	0.81
6	ND	ND	0.88	0.07	1.72	0.04	3.63	0.15	0.31	0.01	2.44	0.03	0.10	0.01	1.79	0.03	19.02	0.23	67.58	0.68
6	ND	ND	0.81	0.07	1.81	0.04	3.24	0.15	0.39	0.01	2.25	0.02	0.11	0.01	1.66	0.02	18.82	0.15	70.76	0.25
6	ND	ND	1.16	0.08	3.17	0.05	1.77	0.17	0.39	0.01	2.62	0.02	0.10	0.01	1.36	0.02	18.48	0.15	70.75	0.27
6	ND	ND	0.89	0.07	3.10	0.05	2.06	0.14	0.43	0.01	1.72	0.02	0.18	0.01	0.54	0.01	12.09	0.14	76.77	0.71
7	ND	ND	1.85	0.07	3.76	0.05	9.46	0.15	0.33	0.01	2.70	0.02	0.11	0.01	1.55	0.02	20.80	0.14	59.30	0.27
7	3.32	0.97	2.69	0.10	6.31	0.10	2.50	0.19	0.40	0.01	3.20	0.04	0.31	0.01	1.87	0.03	21.35	0.26	57.91	0.65
7	ND	ND	1.87	0.08	4.13	0.05	5.26	0.16	0.48	0.01	2.48	0.02	0.15	0.01	1.81	0.02	19.43	0.14	64.29	0.27
7	2.97	0.92	2.31	0.09	4.81	0.07	5.67	0.19	0.66	0.01	2.63	0.03	0.22	0.01	1.93	0.03	19.52	0.23	59.17	0.63
7	ND	ND	1.05	0.08	2.25	0.05	4.41	0.16	0.63	0.01	2.05	0.03	0.15	0.01	1.63	0.02	18.44	0.22	67.10	0.70
7	2.83	0.88	1.11	0.07	2.58	0.05	7.13	0.16	0.50	0.01	2.56	0.03	0.16	0.01	1.46	0.02	18.89	0.21	62.69	0.63
7	ND	ND	0.95	0.07	2.13	0.04	5.68	0.15	0.33	0.01	2.47	0.02	0.24	0.01	1.34	0.02	20.47	0.15	66.30	0.27
8	ND	ND	2.58	0.10	6.01	0.10	ND	ND	0.41	0.01	2.52	0.03	0.16	0.01	1.24	0.02	19.10	0.24	65.25	0.73
8	ND	ND	2.57	0.10	6.03	0.09	2.41	0.18	0.47	0.01	2.62	0.03	0.16	0.01	1.35	0.02	18.38	0.22	63.52	0.66
8	2.95	0.96	3.02	0.11	6.45	0.10	ND	ND	0.46	0.01	2.64	0.03	0.11	0.01	1.51	0.02	18.26	0.22	64.51	0.68
8	ND	ND	2.69	0.10	6.01	0.07	ND	ND	0.51	0.01	2.51	0.02	0.19	0.01	1.56	0.02	18.99	0.14	67.43	0.24
8	ND	ND	1.66	0.08	3.24	0.05	4.10	0.16	0.33	0.01	2.54	0.02	0.10	0.01	1.54	0.02	20.39	0.15	65.98	0.27
8	ND	ND	2.45	0.10	5.44	0.09	ND	ND	0.29	0.01	3.05	0.04	0.24	0.01	1.49	0.02	21.69	0.27	63.07	0.69
8	ND	ND	1.20	0.08	2.92	0.05	2.85	0.15	0.35	0.01	2.80	0.03	0.38	0.01	1.15	0.02	19.33	0.23	66.10	0.68
9	ND	ND	0.76	0.07	1.30	0.03	5.26	0.15	0.28	0.01	2.04	0.03	0.22	0.01	1.38	0.02	18.33	0.22	68.18	0.69
9	ND	ND	0.70	0.07	1.55	0.04	4.13	0.15	0.30	0.01	2.30	0.03	0.12	0.01	1.66	0.02	19.77	0.24	66.68	0.70
9	ND	ND	0.50	0.06	0.98	0.03	5.44	0.14	0.33	0.01	1.85	0.02	0.08	0.01	1.54	0.02	18.29	0.14	70.83	0.24

Continuation of table B9

	Mg	Mg +/-	Al	Al +/-	Si	Si +/-	Cl	Cl +/-	K	K +/-	Ca	Ca +/-	Ti	Ti +/-	Mn	Mn +/-	Fe	Fe +/-	LE	LE +/-
9	ND	ND	0.69	0.07	1.09	0.03	5.09	0.14	0.41	0.01	1.79	0.02	0.16	0.01	1.57	0.02	17.60	0.14	71.51	0.24
9	ND	ND	0.51	0.06	1.08	0.03	5.67	0.15	0.52	0.01	1.47	0.02	0.15	0.01	1.49	0.02	15.47	0.18	71.19	0.70
9	ND	ND	0.64	0.06	1.16	0.03	5.98	0.15	0.48	0.01	1.30	0.02	0.10	0.01	1.41	0.02	16.10	0.19	70.42	0.68
9	2.84	0.86	0.86	0.07	1.73	0.04	5.78	0.15	0.44	0.01	1.93	0.02	0.11	0.01	1.57	0.02	17.65	0.20	66.96	0.64
9	ND	ND	1.65	0.08	3.46	0.06	3.18	0.16	0.48	0.01	2.32	0.03	0.18	0.01	1.43	0.02	18.87	0.22	65.68	0.66
10	ND	ND	0.59	0.07	1.65	0.04	5.65	0.16	0.52	0.01	1.90	0.02	0.13	0.01	1.22	0.02	15.83	0.19	69.96	0.71
10	3.53	0.95	0.83	0.07	2.50	0.05	4.77	0.16	0.48	0.01	2.08	0.03	0.08	0.01	1.51	0.02	17.05	0.21	67.07	0.71
10	ND	ND	1.16	0.07	3.20	0.05	3.06	0.15	0.47	0.01	2.64	0.02	0.13	0.01	1.76	0.02	18.72	0.14	68.78	0.26
10	ND	ND	1.24	0.08	3.26	0.05	4.33	0.16	0.50	0.01	2.58	0.02	0.12	0.01	1.72	0.02	18.16	0.14	67.94	0.26
10	ND	ND	1.35	0.08	3.26	0.05	3.26	0.15	0.34	0.01	2.80	0.02	0.16	0.01	1.81	0.02	18.91	0.14	67.98	0.26
10	ND	ND	1.14	0.07	2.81	0.04	4.06	0.15	0.41	0.01	2.60	0.02	0.15	0.01	1.80	0.02	19.01	0.14	67.91	0.26
10	ND	ND	1.01	0.07	2.75	0.05	4.24	0.16	0.46	0.01	2.70	0.03	0.14	0.01	1.66	0.02	19.01	0.23	65.26	0.68
10	ND	ND	1.32	0.08	3.51	0.05	2.39	0.15	0.39	0.01	2.70	0.02	0.44	0.01	1.52	0.02	19.86	0.15	67.72	0.26
11	ND	ND	1.34	0.11	6.27	0.09	ND	ND	0.79	0.01	2.28	0.02	0.13	0.01	1.10	0.02	14.11	0.13	73.82	0.24
11	ND	ND	2.54	0.10	8.06	0.09	ND	ND	0.50	0.01	3.17	0.02	0.20	0.01	1.39	0.02	15.93	0.12	67.94	0.24
11	ND	ND	2.19	0.10	7.41	0.08	ND	ND	0.62	0.01	2.81	0.02	0.14	0.01	1.79	0.02	17.93	0.14	66.96	0.26
11	ND	ND	2.68	0.11	8.21	0.09	ND	ND	0.54	0.01	3.04	0.02	0.23	0.01	2.08	0.02	20.55	0.15	62.48	0.28
11	ND	ND	3.10	0.11	10.96	0.10	ND	ND	0.64	0.01	3.18	0.02	0.23	0.01	2.03	0.02	19.88	0.14	59.81	0.28
11	ND	ND	2.76	0.10	10.71	0.14	2.12	0.21	0.73	0.01	3.03	0.04	0.19	0.01	1.75	0.03	20.11	0.23	56.02	0.59
11	ND	ND	3.12	0.09	7.94	0.08	6.07	0.18	0.37	0.01	3.77	0.03	0.11	0.01	1.66	0.02	22.51	0.14	54.28	0.29
12	ND	ND	1.81	0.09	3.25	0.06	ND	ND	0.31	0.01	2.45	0.03	0.15	0.01	1.39	0.02	19.48	0.26	68.68	0.78
12	ND	ND	1.49	0.08	3.51	0.05	1.18	0.16	0.41	0.01	2.26	0.02	0.15	0.01	1.58	0.02	17.20	0.13	72.04	0.25
12	3.31	1.05	1.77	0.09	3.80	0.07	ND	ND	0.33	0.01	2.63	0.04	0.27	0.01	2.05	0.03	20.49	0.27	65.10	0.75
12	ND	ND	1.42	0.08	3.33	0.05	ND	ND	0.35	0.01	2.23	0.02	0.16	0.01	1.87	0.02	18.73	0.15	71.65	0.23

Continuation of table B9

	Mg	Mg +/-	Al	Al +/-	Si	Si +/-	Cl	Cl +/-	K	K +/-	Ca	Ca +/-	Ti	Ti +/-	Mn	Mn +/-	Fe	Fe +/-	LE	LE +/-
12	3.64	1.03	1.14	0.08	2.15	0.05	3.09	0.17	0.40	0.01	2.05	0.03	0.12	0.01	1.75	0.03	18.19	0.24	67.27	0.77
12	ND	ND	1.08	0.08	2.00	0.04	2.81	0.15	0.46	0.01	1.68	0.02	0.10	0.01	1.60	0.02	16.40	0.13	73.65	0.24
12	ND	ND	1.50	0.08	3.02	0.06	1.34	0.16	0.39	0.01	2.17	0.03	0.24	0.01	1.83	0.03	18.94	0.23	68.01	0.71
12	ND	ND	1.21	0.08	2.36	0.04	2.58	0.15	0.41	0.01	2.23	0.02	0.18	0.01	1.56	0.02	19.08	0.15	70.13	0.25
12	ND	ND	1.17	0.08	2.50	0.05	2.96	0.16	0.44	0.01	2.36	0.03	0.17	0.01	1.25	0.02	18.15	0.23	68.01	0.73
13	3.45	1.11	1.99	0.10	4.61	0.08	ND	ND	0.22	0.01	2.86	0.04	0.08	0.01	1.69	0.03	20.48	0.28	64.47	0.79
13	ND	ND	2.49	0.10	5.95	0.07	ND	ND	0.41	0.01	3.03	0.02	0.14	0.01	2.08	0.02	20.40	0.15	65.33	0.26
13	2.98	0.95	2.75	0.10	6.95	0.10	ND	ND	0.35	0.01	3.37	0.04	0.11	0.01	2.35	0.03	21.69	0.26	59.28	0.64
13	ND	ND	2.33	0.09	6.23	0.07	ND	ND	0.31	0.01	2.81	0.02	0.10	0.01	2.13	0.02	19.74	0.14	66.21	0.25
13	ND	ND	2.28	0.11	6.63	0.08	ND	ND	0.39	0.01	3.19	0.03	0.17	0.01	2.15	0.03	20.30	0.17	64.73	0.29
13	ND	ND	1.76	0.15	5.59	0.10	ND	ND	0.35	0.01	3.78	0.05	0.10	0.01	1.52	0.03	19.64	0.23	67.15	0.39
14	3.45	1.05	1.33	0.09	3.34	0.06	3.49	0.18	0.44	0.01	3.41	0.05	0.14	0.01	1.53	0.03	20.36	0.27	62.36	0.74
14	ND	ND	0.92	0.08	2.36	0.05	6.21	0.20	0.39	0.01	2.79	0.04	0.15	0.01	1.58	0.03	18.02	0.25	64.62	0.81
14	ND	ND	1.12	0.08	3.28	0.06	4.19	0.18	0.34	0.01	2.97	0.04	0.15	0.01	1.96	0.03	19.35	0.26	63.80	0.76
14	ND	ND	1.27	0.08	3.44	0.05	2.09	0.17	0.44	0.01	2.65	0.02	0.14	0.01	1.89	0.02	18.18	0.14	69.76	0.27
14	ND	ND	1.31	0.08	3.59	0.05	2.56	0.17	0.39	0.01	2.87	0.02	0.09	0.01	2.00	0.02	19.26	0.15	67.74	0.27
14	ND	ND	1.00	0.07	2.82	0.05	3.00	0.15	0.44	0.01	2.69	0.02	0.28	0.01	1.86	0.02	18.13	0.14	69.63	0.26
14	ND	ND	0.94	0.07	2.94	0.05	3.01	0.15	0.44	0.01	2.67	0.02	0.11	0.01	1.57	0.02	16.97	0.13	71.20	0.25
14	ND	ND	1.18	0.09	3.46	0.07	3.00	0.19	0.49	0.01	3.16	0.04	0.18	0.01	1.35	0.02	18.93	0.26	65.51	0.80
15	ND	ND	2.11	0.09	4.70	0.06	2.28	0.17	0.26	0.01	3.30	0.03	0.11	0.01	1.71	0.02	20.92	0.16	64.41	0.28
15	ND	ND	1.53	0.08	3.69	0.07	2.31	0.17	0.22	0.01	2.84	0.04	0.11	0.01	1.91	0.03	20.86	0.26	63.47	0.71
15	ND	ND	1.09	0.07	2.24	0.04	5.03	0.15	0.21	0.01	2.53	0.02	0.11	0.01	1.95	0.02	19.44	0.14	67.21	0.26
15	ND	ND	1.81	0.08	3.95	0.05	3.83	0.16	0.21	0.01	2.86	0.02	0.18	0.01	2.01	0.02	20.54	0.15	64.42	0.28
15	ND	ND	1.53	0.07	3.72	0.05	8.87	0.16	0.30	0.01	2.97	0.02	0.18	0.01	2.01	0.02	20.28	0.14	59.99	0.28

Continuation of table B9

	Mg	Mg +/-	Al	Al +/-	Si	Si +/-	Cl	Cl +/-	K	K +/-	Ca	Ca +/-	Ti	Ti +/-	Mn	Mn +/-	Fe	Fe +/-	LE	LE +/-
15	ND	ND	1.61	0.08	3.85	0.06	4.33	0.17	0.22	0.01	2.85	0.03	0.15	0.01	1.93	0.03	20.51	0.24	61.91	0.63
15	ND	ND	1.74	0.08	4.30	0.07	3.58	0.17	0.37	0.01	2.96	0.04	0.10	0.01	1.84	0.03	20.77	0.24	61.66	0.63
15	ND	ND	1.70	0.08	4.00	0.07	2.57	0.16	0.32	0.01	2.62	0.03	0.10	0.01	1.40	0.02	21.48	0.25	63.59	0.66
15	ND	ND	1.00	0.07	1.96	0.04	5.57	0.15	0.32	0.01	2.21	0.03	0.13	0.01	1.12	0.02	20.07	0.23	64.91	0.64

Table B10: The table presents the data of the cross-section from the XRF-analysis of the graded bed at locality A. The elements are given in wt.% with their respective standard error. ND is an abbreviation for "No Data".

XRF-measurements of a graded bed

Distance	wt.% element																			
(cm)	Mg	Mg +/-	Al	Al +/-	Si	Si +/-	Cl	Cl +/-	K	K +/-	Ca	Ca +/-	Ti	Ti +/-	Mn	Mn +/-	Fe	Fe +/-	LE	LE +/-
1	ND	ND	1.28	0.07	3.98	0.06	3.73	0.15	0.35	0.01	3.95	0.04	0.28	0.01	0.06	0.00	4.99	0.05	79.28	0.68
2	ND	ND	0.99	0.07	3.43	0.05	5.08	0.14	0.48	0.01	3.73	0.04	0.25	0.01	0.07	0.00	5.37	0.06	78.45	0.66
3	ND	ND	0.65	0.06	2.45	0.04	4.68	0.13	0.38	0.01	3.20	0.02	0.23	0.01	0.07	0.00	5.36	0.04	82.76	0.17
4	ND	ND	0.82	0.07	2.65	0.05	4.30	0.14	0.50	0.01	2.63	0.03	0.19	0.01	0.24	0.01	8.31	0.09	78.05	0.71
5	ND	ND	0.99	0.06	3.84	0.06	6.24	0.15	0.43	0.01	3.44	0.04	0.26	0.01	0.09	0.00	7.27	0.08	75.19	0.63
6	ND	ND	0.81	0.06	3.22	0.05	4.64	0.14	0.41	0.01	3.25	0.04	0.32	0.01	0.18	0.01	9.32	0.10	75.20	0.67
7	ND	ND	0.69	0.06	4.06	0.06	4.27	0.15	0.39	0.01	2.94	0.03	0.26	0.01	0.44	0.01	12.44	0.14	71.94	0.65
8	ND	ND	0.37	0.06	1.72	0.03	5.62	0.14	0.41	0.01	2.22	0.02	0.23	0.01	0.44	0.01	13.40	0.10	75.37	0.21
9	ND	ND	0.46	0.06	1.78	0.04	5.25	0.15	0.38	0.01	2.37	0.03	0.21	0.01	0.26	0.01	10.24	0.12	76.43	0.74
10	ND	ND	0.22	0.05	1.35	0.03	5.73	0.13	0.40	0.01	2.48	0.02	0.19	0.01	0.22	0.01	9.37	0.07	79.85	0.18
11	ND	ND	0.37	0.06	1.21	0.03	5.91	0.13	0.44	0.01	2.31	0.02	0.23	0.01	0.30	0.01	11.09	0.08	77.93	0.19
12	ND	ND	0.63	0.06	2.26	0.04	4.67	0.14	0.35	0.01	2.82	0.02	0.21	0.01	0.27	0.01	9.41	0.07	79.14	0.19
13	ND	ND	0.75	0.06	2.09	0.04	5.05	0.15	0.36	0.01	2.82	0.03	0.27	0.01	0.31	0.01	9.32	0.11	76.86	0.73
14	2.85	0.88	0.57	0.06	1.91	0.04	5.09	0.15	0.40	0.01	3.19	0.04	0.28	0.01	0.09	0.00	8.18	0.09	77.22	0.72
15	3.84	0.88	0.44	0.06	1.56	0.03	5.39	0.14	0.40	0.01	2.20	0.03	0.20	0.01	0.11	0.00	6.96	0.08	78.69	0.74
16	ND	ND	0.41	0.06	2.12	0.04	5.20	0.14	0.35	0.01	2.57	0.02	0.21	0.01	0.10	0.00	5.51	0.04	83.35	0.17
17	ND	ND	0.34	0.06	1.50	0.03	5.52	0.14	0.43	0.01	2.31	0.02	0.29	0.01	0.18	0.01	9.80	0.07	79.39	0.19
18	ND	ND	0.94	0.07	3.14	0.04	3.80	0.15	0.36	0.01	3.36	0.02	0.20	0.01	0.07	0.00	6.13	0.05	81.78	0.18
19	ND	ND	0.74	0.06	2.71	0.05	3.95	0.14	0.33	0.01	3.39	0.04	0.40	0.01	0.25	0.01	9.02	0.10	77.06	0.72
20	ND	ND	1.37	0.08	4.55	0.07	2.70	0.16	0.32	0.01	3.65	0.04	0.19	0.01	0.22	0.01	7.37	0.09	77.43	0.74
21	ND	ND	1.27	0.07	4.30	0.05	2.60	0.15	0.36	0.01	3.83	0.03	0.28	0.01	0.08	0.00	6.70	0.05	80.35	0.19

Continuation of table B10

	Mg	Mg +/-	Al	Al +/-	Si	Si +/-	Cl	Cl +/-	K	K +/-	Ca	Ca +/-	Ti	Ti +/-	Mn	Mn +/-	Fe	Fe +/-	LE	LE +/-
22	ND	ND	1.36	0.07	4.48	0.05	2.98	0.16	0.25	0.01	3.87	0.03	0.17	0.01	0.05	0.00	3.37	0.03	83.28	0.18
23	ND	ND	0.59	0.06	2.77	0.04	4.73	0.14	0.28	0.01	3.48	0.02	0.26	0.01	0.07	0.00	5.09	0.04	82.52	0.17
24	ND	ND	0.33	0.05	1.33	0.03	6.36	0.14	0.32	0.01	2.95	0.03	0.27	0.01	0.08	0.00	5.69	0.06	80.44	0.72
25	3.21	0.94	0.39	0.06	1.86	0.04	5.74	0.16	0.30	0.01	2.51	0.03	0.22	0.01	0.34	0.01	12.33	0.15	72.88	0.74
26	ND	ND	0.49	0.07	1.92	0.04	5.90	0.18	0.38	0.01	2.86	0.04	0.30	0.01	0.09	0.00	6.28	0.09	78.57	0.89
27	2.82	0.92	0.36	0.06	1.23	0.03	5.75	0.15	0.38	0.01	1.51	0.02	0.12	0.01	0.35	0.01	10.40	0.12	76.89	0.75
28	2.99	0.92	0.28	0.06	0.60	0.02	6.92	0.15	0.41	0.01	1.26	0.02	0.12	0.01	0.16	0.01	7.73	0.09	79.31	0.78
29	2.83	0.86	0.18	0.05	0.63	0.02	7.11	0.15	0.36	0.01	1.28	0.02	0.17	0.01	0.26	0.01	11.38	0.13	75.57	0.69
30	ND	ND	0.30	0.06	0.53	0.02	6.95	0.16	0.28	0.01	1.25	0.02	0.16	0.01	0.30	0.01	11.89	0.15	75.33	0.77
31	ND	ND	ND	ND	0.43	0.02	6.63	0.15	0.24	0.01	0.99	0.01	0.18	0.01	0.25	0.01	11.64	0.14	77.44	0.74
32	ND	ND	0.31	0.05	0.67	0.02	6.57	0.14	0.50	0.01	1.42	0.02	0.21	0.01	0.32	0.01	12.21	0.14	75.42	0.69
33	ND	ND	0.20	0.05	0.50	0.02	7.30	0.13	0.32	0.01	0.91	0.01	0.09	0.01	0.32	0.01	10.09	0.08	80.08	0.18
34	ND	ND	0.21	0.05	0.40	0.02	7.30	0.15	0.42	0.01	0.54	0.01	0.08	0.01	0.05	0.00	4.61	0.05	83.56	0.77
35	3.74	0.97	0.61	0.07	1.82	0.04	4.80	0.16	0.43	0.01	1.51	0.02	0.24	0.01	0.38	0.01	10.76	0.14	75.46	0.79
36	ND	ND	0.23	0.06	0.53	0.02	7.29	0.15	0.37	0.01	1.14	0.01	0.18	0.01	0.08	0.00	7.03	0.06	82.92	0.18
37	ND	ND	0.18	0.05	0.68	0.02	7.11	0.14	0.36	0.01	2.15	0.02	0.18	0.01	0.08	0.00	6.96	0.05	82.06	0.18
38	ND	ND	0.24	0.05	0.95	0.03	5.98	0.15	0.33	0.01	1.60	0.02	0.18	0.01	0.52	0.01	11.33	0.13	76.69	0.73
39	ND	ND	0.49	0.06	1.35	0.03	5.25	0.14	0.32	0.01	2.16	0.03	0.21	0.01	0.29	0.01	8.23	0.09	79.38	0.73
40	ND	ND	0.82	0.06	2.49	0.04	4.71	0.15	0.35	0.01	3.54	0.04	0.22	0.01	0.05	0.00	5.65	0.06	79.71	0.72
41	2.64	0.84	0.57	0.06	2.31	0.04	5.00	0.14	0.36	0.01	3.31	0.04	0.16	0.01	0.06	0.00	5.39	0.06	79.97	0.71
42	ND	ND	0.50	0.06	7.98	0.07	2.36	0.16	0.26	0.01	2.59	0.02	0.19	0.01	0.03	0.00	2.59	0.02	83.34	0.19
43	ND	ND	0.39	0.05	2.43	0.04	5.44	0.13	0.30	0.01	2.46	0.02	0.14	0.01	0.09	0.00	5.01	0.04	83.51	0.16
44	2.65	0.87	0.55	0.06	2.15	0.04	5.65	0.15	0.29	0.01	2.45	0.03	0.11	0.01	0.12	0.00	4.97	0.06	80.86	0.75
45	ND	ND	0.30	0.05	1.14	0.03	6.23	0.13	0.36	0.01	2.89	0.02	0.18	0.01	0.06	0.00	5.27	0.04	83.38	0.16
46	ND	ND	0.37	0.06	1.44	0.03	6.19	0.13	0.41	0.01	2.68	0.02	0.18	0.01	0.05	0.00	5.01	0.04	83.42	0.16

Continuation of table B10

	Mg	Mg +/-	Al	Al +/-	Si	Si +/-	Cl	Cl +/-	K	K +/-	Ca	Ca +/-	Ti	Ti +/-	Mn	Mn +/-	Fe	Fe +/-	LE	LE +/-
47	ND	ND	0.27	0.05	0.74	0.02	6.82	0.14	0.41	0.01	1.52	0.02	0.13	0.01	0.21	0.01	10.13	0.11	77.46	0.70
48	ND	ND	0.16	0.05	0.40	0.02	6.76	0.15	0.48	0.01	0.58	0.01	0.13	0.01	0.09	0.00	6.48	0.08	82.41	0.79
49	ND	ND	0.24	0.05	0.65	0.02	6.51	0.13	0.51	0.01	0.92	0.01	0.08	0.01	0.14	0.00	6.42	0.05	84.30	0.16
50	ND	ND	ND	ND	0.41	0.02	6.41	0.14	0.31	0.01	1.64	0.01	0.17	0.01	0.23	0.01	11.38	0.09	79.05	0.20
51	ND	ND	ND	ND	0.38	0.02	5.70	0.14	0.25	0.01	1.19	0.01	0.17	0.01	0.42	0.01	13.47	0.11	78.02	0.21
52	ND	ND	ND	ND	1.41	0.04	5.01	0.16	0.27	0.01	1.60	0.02	0.19	0.01	0.26	0.01	11.42	0.09	79.67	0.20
53	ND	ND	0.33	0.05	0.92	0.03	6.25	0.14	0.34	0.01	1.72	0.02	0.23	0.01	0.41	0.01	14.21	0.16	73.23	0.68
54	ND	ND	0.32	0.05	2.13	0.04	5.58	0.13	0.33	0.01	1.94	0.02	0.18	0.01	0.34	0.01	11.89	0.09	77.08	0.20
55	ND	ND	0.38	0.05	1.39	0.03	6.24	0.13	0.34	0.01	1.61	0.01	0.15	0.01	0.34	0.01	12.65	0.09	76.69	0.20
56	ND	ND	ND	ND	0.40	0.02	6.83	0.14	0.35	0.01	1.48	0.02	0.17	0.01	0.31	0.01	11.87	0.13	76.08	0.67
57	4.22	0.97	0.23	0.06	0.40	0.02	6.96	0.16	0.41	0.01	0.79	0.01	0.12	0.01	0.25	0.01	9.60	0.12	76.80	0.81
58	ND	ND	0.21	0.06	0.65	0.02	6.26	0.16	0.46	0.01	0.89	0.01	0.09	0.01	0.13	0.01	6.38	0.05	84.72	0.19
59	ND	ND	0.24	0.07	0.85	0.03	6.54	0.17	0.53	0.01	1.19	0.01	0.18	0.01	0.06	0.00	4.97	0.04	85.18	0.19
60	ND	ND	1.03	0.08	3.26	0.06	4.08	0.17	0.46	0.01	2.73	0.04	0.17	0.01	0.06	0.00	4.29	0.06	81.36	0.87

Table B11: The table presents the data of the cross-section from the XRF-analysis of the alterations at locality B. The elements are given in wt.% with their respective standard error. ND is an abbreviation for "No Data".

XRF-measurements of alterations at Locality B

Alteration	wt.% element																			
number	Mg	Mg +/-	Al	Al +/-	Si	Si +/-	Cl	Cl +/-	K	K +/-	Ca	Ca +/-	Ti	Ti +/-	Mn	Mn +/-	Fe	Fe +/-	LE	LE +/-
1	ND	ND	1.57	0.07	6.37	0.06	5.03	0.15	0.42	0.01	3.67	0.02	0.20	0.01	0.06	0.00	5.06	0.04	77.36	0.19
1	ND	ND	2.02	0.08	7.05	0.07	2.58	0.17	0.47	0.01	3.86	0.03	0.19	0.01	0.08	0.00	5.20	0.04	78.28	0.20
1	ND	ND	1.62	0.08	6.74	0.07	ND	ND	0.56	0.01	3.71	0.03	0.27	0.01	0.12	0.00	8.19	0.06	78.50	0.16
1	2.72	0.89	2.70	0.10	10.06	0.13	ND	ND	0.76	0.01	3.95	0.04	0.20	0.01	0.10	0.00	5.70	0.07	73.54	0.70
1	ND	ND	2.65	0.10	11.00	0.09	ND	ND	1.92	0.02	3.32	0.02	0.16	0.01	0.12	0.00	5.02	0.04	75.55	0.17
1	ND	ND	2.76	0.10	11.32	0.09	ND	ND	3.29	0.02	2.30	0.02	0.15	0.01	0.11	0.00	5.35	0.04	74.43	0.17
1	ND	ND	3.69	0.10	13.36	0.10	ND	ND	1.32	0.01	3.92	0.02	0.36	0.01	0.08	0.00	4.18	0.03	72.91	0.17
1	ND	ND	4.30	0.10	15.01	0.10	ND	ND	0.57	0.01	4.87	0.03	0.35	0.01	0.09	0.00	5.12	0.03	69.44	0.18
1	ND	ND	3.25	0.09	12.56	0.10	ND	ND	0.48	0.01	4.42	0.03	0.18	0.01	0.12	0.00	4.52	0.03	74.25	0.16
1	ND	ND	2.73	0.09	9.68	0.08	ND	ND	0.66	0.01	4.34	0.03	0.19	0.01	0.09	0.00	5.38	0.04	76.66	0.16
1	ND	ND	2.92	0.09	10.31	0.09	ND	ND	0.63	0.01	4.54	0.03	0.25	0.01	0.12	0.00	6.62	0.04	74.32	0.17
2	ND	ND	1.89	0.08	7.67	0.07	ND	ND	0.42	0.01	3.83	0.03	0.16	0.01	0.09	0.00	4.99	0.04	80.71	0.14
2	ND	ND	3.12	0.09	11.15	0.09	ND	ND	0.54	0.01	4.95	0.03	0.25	0.01	0.10	0.00	6.24	0.04	73.40	0.17
2	ND	ND	3.17	0.09	10.35	0.08	ND	ND	0.74	0.01	4.97	0.03	0.20	0.01	0.10	0.00	5.58	0.04	74.67	0.17
2	ND	ND	2.91	0.09	10.61	0.09	ND	ND	0.72	0.01	4.49	0.03	0.20	0.01	0.09	0.00	5.29	0.04	75.47	0.16
2	ND	ND	3.26	0.09	11.76	0.09	ND	ND	1.40	0.01	4.31	0.03	0.18	0.01	0.08	0.00	4.64	0.03	74.14	0.16
2	ND	ND	2.81	0.10	10.94	0.09	ND	ND	3.52	0.02	5.97	0.04	0.23	0.01	0.11	0.00	5.58	0.04	70.60	0.18
2	ND	ND	2.91	0.10	10.96	0.09	ND	ND	2.98	0.02	3.67	0.02	0.21	0.01	0.10	0.00	5.09	0.04	73.85	0.17
2	ND	ND	3.46	0.10	12.65	0.09	ND	ND	1.91	0.01	4.18	0.03	0.19	0.01	0.08	0.00	4.19	0.03	73.12	0.17
2	ND	ND	2.59	0.09	9.33	0.08	ND	ND	1.12	0.01	4.21	0.03	0.20	0.01	0.10	0.00	5.77	0.04	76.46	0.16

Continuation of table B11

	Mg	Mg +/-	Al	Al +/-	Si	Si +/-	Cl	Cl +/-	K	K +/-	Ca	Ca +/-	Ti	Ti +/-	Mn	Mn +/-	Fe	Fe +/-	LE	LE +/-
2	ND	ND	2.83	0.10	10.46	0.12	ND	ND	1.27	0.02	4.35	0.05	0.22	0.01	0.08	0.00	4.87	0.05	73.40	0.64
2	ND	ND	2.31	0.09	8.82	0.08	ND	ND	0.74	0.01	4.26	0.03	0.21	0.01	0.15	0.01	6.96	0.05	76.34	0.16
3	ND	ND	0.88	0.06	2.85	0.04	4.01	0.13	0.39	0.01	1.81	0.02	0.11	0.01	0.09	0.00	8.87	0.09	78.59	0.62
3	ND	ND	1.26	0.07	5.12	0.06	2.78	0.15	0.52	0.01	3.20	0.02	0.21	0.01	0.04	0.00	3.33	0.03	83.33	0.18
3	ND	ND	1.00	0.07	4.18	0.05	3.98	0.14	0.41	0.01	2.10	0.02	0.16	0.01	0.04	0.00	3.42	0.03	84.52	0.17
3	3.55	0.87	1.16	0.07	4.16	0.06	3.08	0.15	0.56	0.01	2.66	0.03	0.21	0.01	0.06	0.00	3.79	0.04	80.54	0.75
3	ND	ND	0.99	0.07	3.92	0.06	3.69	0.15	1.21	0.02	2.39	0.03	0.18	0.01	0.04	0.00	4.02	0.05	81.24	0.74
3	ND	ND	1.21	0.08	4.60	0.05	2.66	0.16	1.18	0.01	2.48	0.02	0.17	0.01	0.05	0.00	3.80	0.03	83.64	0.18
3	ND	ND	1.68	0.08	5.47	0.06	1.91	0.16	0.80	0.01	3.59	0.02	0.31	0.01	0.05	0.00	4.11	0.03	81.85	0.19
3	ND	ND	1.88	0.08	6.08	0.06	3.05	0.16	0.43	0.01	4.13	0.03	0.22	0.01	0.06	0.00	6.00	0.04	77.91	0.19
3	ND	ND	1.59	0.08	5.79	0.06	1.28	0.16	0.40	0.01	4.48	0.03	0.32	0.01	0.04	0.00	3.37	0.03	82.51	0.18
3	ND	ND	1.42	0.07	4.98	0.06	2.73	0.16	0.43	0.01	3.61	0.02	0.24	0.01	0.04	0.00	3.27	0.03	83.06	0.18
3	ND	ND	1.29	0.07	5.08	0.07	2.95	0.16	0.49	0.01	3.49	0.04	0.19	0.01	0.06	0.00	5.46	0.06	78.75	0.70
4	3.15	0.91	1.92	0.09	7.56	0.10	ND	ND	0.70	0.01	3.74	0.04	0.18	0.01	0.07	0.00	3.96	0.05	78.49	0.75
4	ND	ND	1.97	0.08	7.62	0.07	ND	ND	0.45	0.01	4.26	0.03	0.18	0.01	0.06	0.00	3.02	0.02	82.19	0.13
4	ND	ND	2.10	0.08	8.37	0.08	ND	ND	0.35	0.01	3.90	0.03	0.14	0.01	0.14	0.00	4.56	0.03	80.21	0.14
4	ND	ND	1.49	0.08	6.13	0.07	1.36	0.17	0.60	0.01	3.67	0.03	0.17	0.01	0.07	0.00	3.41	0.03	82.93	0.19
4	ND	ND	1.33	0.08	5.09	0.06	1.67	0.16	1.17	0.01	3.40	0.02	0.14	0.01	0.06	0.00	3.17	0.03	83.75	0.19
4	ND	ND	0.62	0.08	2.75	0.05	4.28	0.15	2.97	0.03	2.12	0.02	0.11	0.01	0.10	0.00	5.17	0.06	79.58	0.72
4	ND	ND	2.31	0.09	8.97	0.08	ND	ND	1.77	0.01	3.66	0.02	0.16	0.01	0.08	0.00	3.78	0.03	79.07	0.15
4	ND	ND	2.54	0.09	9.29	0.08	ND	ND	0.89	0.01	4.38	0.03	0.23	0.01	0.11	0.00	6.75	0.05	75.55	0.17
4	ND	ND	2.22	0.08	8.37	0.08	ND	ND	0.76	0.01	4.14	0.03	0.23	0.01	0.07	0.00	4.93	0.03	79.05	0.15
4	ND	ND	1.66	0.08	6.22	0.06	2.32	0.16	0.48	0.01	4.05	0.03	0.21	0.01	0.06	0.00	3.81	0.03	80.96	0.19
4	ND	ND	1.28	0.08	6.06	0.06	ND	ND	0.51	0.01	3.76	0.03	0.24	0.01	0.14	0.00	7.98	0.06	79.77	0.15

Continuation of table B11

	Mg	Mg +/-	Al	Al +/-	Si	Si +/-	Cl	Cl +/-	K	K +/-	Ca	Ca +/-	Ti	Ti +/-	Mn	Mn +/-	Fe	Fe +/-	LE	LE +/-
5	ND	ND	0.91	0.07	3.00	0.04	4.65	0.15	0.43	0.01	4.01	0.03	0.13	0.01	0.04	0.00	2.07	0.02	84.58	0.17
5	ND	ND	1.48	0.08	4.65	0.07	3.75	0.16	0.53	0.01	3.73	0.04	0.22	0.01	0.05	0.00	3.33	0.04	80.07	0.72
5	ND	ND	1.20	0.07	4.01	0.06	3.70	0.15	0.52	0.01	3.99	0.04	0.16	0.01	0.04	0.00	2.85	0.03	81.31	0.74
5	ND	ND	1.77	0.08	5.34	0.07	1.61	0.16	0.92	0.01	4.37	0.05	0.17	0.01	0.07	0.00	3.56	0.04	80.06	0.72
5	ND	ND	2.09	0.09	7.09	0.09	ND	ND	2.01	0.02	4.70	0.05	0.19	0.01	0.05	0.00	2.20	0.03	79.68	0.72
5	ND	ND	0.89	0.08	3.43	0.05	3.02	0.16	3.22	0.04	2.69	0.03	0.25	0.01	0.11	0.00	7.00	0.08	77.37	0.70
5	ND	ND	1.04	0.08	3.88	0.05	2.61	0.15	2.28	0.02	3.02	0.02	0.28	0.01	0.10	0.00	6.58	0.05	79.98	0.19
5	ND	ND	0.98	0.07	3.04	0.04	3.59	0.14	0.64	0.01	2.85	0.02	0.26	0.01	0.74	0.01	14.29	0.10	73.42	0.22
5	ND	ND	0.64	0.06	2.33	0.04	4.98	0.15	0.58	0.01	3.09	0.03	0.25	0.01	0.08	0.00	5.29	0.06	80.13	0.73
5	ND	ND	0.91	0.07	2.95	0.04	4.46	0.14	0.42	0.01	3.82	0.03	0.22	0.01	0.04	0.00	3.65	0.03	83.31	0.17
5	ND	ND	0.76	0.06	2.62	0.04	6.13	0.14	0.44	0.01	2.91	0.02	0.18	0.01	0.04	0.00	3.39	0.03	83.34	0.17

Table B12: The table presents the data of the cross-section from the XRF-analysis of the alterations at locality B. The elements are given in wt.% with their respective standard error. ND is an abbreviation for "No Data".

XRF-measurements of alterations at Locality C

Alteration	wt.% element																	
nr	Al	Al +/-	Si	Si +/-	P	P +/-	K	K +/-	Ca	Ca +/-	Ti	Ti +/-	Mn	Mn +/-	Fe	Fe +/-	LE	LE +/-
1	2.30	0.09	8.07	0.10	ND	ND	0.70	0.01	4.92	0.05	0.31	0.01	0.11	0.00	6.40	0.07	75.27	0.66
1	2.80	0.09	9.25	0.08	ND	ND	0.83	0.01	5.55	0.04	0.37	0.01	0.13	0.00	7.31	0.05	73.53	0.18
1	3.43	0.09	11.77	0.09	0.05	0.01	0.94	0.01	5.89	0.04	0.54	0.01	0.11	0.00	6.10	0.04	70.95	0.18
1	3.71	0.09	12.93	0.09	0.04	0.01	1.56	0.01	6.95	0.04	0.57	0.02	0.12	0.00	6.60	0.04	67.30	0.19
1	2.96	0.10	11.54	0.09	0.06	0.01	4.67	0.03	4.14	0.03	0.36	0.01	0.10	0.00	6.56	0.04	69.38	0.19
1	2.33	0.10	10.01	0.08	ND	ND	4.78	0.03	4.17	0.03	0.37	0.01	0.10	0.00	5.69	0.04	72.32	0.18
1	2.34	0.09	8.73	0.08	ND	ND	1.68	0.01	5.48	0.04	0.31	0.01	0.11	0.00	6.77	0.05	74.36	0.17
1	3.23	0.09	11.20	0.09	ND	ND	0.93	0.01	6.28	0.04	0.52	0.01	0.11	0.00	5.77	0.04	71.76	0.18
1	3.06	0.09	10.97	0.12	ND	ND	0.69	0.01	5.95	0.06	0.40	0.01	0.12	0.00	7.02	0.07	69.72	0.57
1	1.83	0.09	7.23	0.07	ND	ND	0.73	0.01	4.12	0.03	0.38	0.01	0.08	0.00	4.29	0.03	81.17	0.14
1	2.31	0.09	8.25	0.08	ND	ND	1.48	0.01	5.24	0.03	0.29	0.01	0.07	0.00	4.22	0.03	77.93	0.16
2	3.33	0.10	9.04	0.11	ND	ND	0.37	0.01	4.51	0.05	0.26	0.01	0.11	0.00	6.58	0.07	73.38	0.65
2	3.82	0.10	11.18	0.09	ND	ND	0.51	0.01	5.82	0.04	0.24	0.01	0.12	0.00	6.31	0.04	71.78	0.19
2	4.02	0.11	11.26	0.13	ND	ND	0.38	0.01	6.08	0.06	0.45	0.01	0.12	0.00	6.93	0.07	68.67	0.60
2	3.98	0.10	11.56	0.09	ND	ND	0.82	0.01	5.70	0.04	0.36	0.01	0.12	0.00	6.60	0.04	70.63	0.19
2	3.49	0.10	11.72	0.10	ND	ND	1.46	0.01	4.26	0.03	0.44	0.01	0.14	0.01	7.57	0.05	70.69	0.19
2	4.44	0.10	16.02	0.11	0.21	0.01	1.13	0.01	2.89	0.02	0.47	0.01	0.13	0.00	6.44	0.04	68.04	0.19
2	4.19	0.11	14.45	0.16	0.08	0.01	1.34	0.02	3.86	0.04	0.47	0.01	0.14	0.01	8.09	0.08	65.38	0.57
2	4.73	0.11	15.42	0.11	0.08	0.01	1.63	0.01	6.08	0.04	0.45	0.01	0.15	0.01	8.74	0.05	62.45	0.22
2	4.78	0.11	14.09	0.10	ND	ND	1.94	0.01	5.19	0.03	0.33	0.01	0.12	0.00	6.46	0.04	66.87	0.20

Continuation of table B12

	Al	Al +/-	Si	Si +/-	P	P +/-	K	K +/-	Ca	Ca +/-	Ti	Ti +/-	Mn	Mn +/-	Fe	Fe +/-	LE	LE +/-
2	5.45	0.11	15.84	0.11	0.04	0.01	1.85	0.01	5.66	0.03	0.42	0.01	0.15	0.01	7.55	0.05	62.81	0.21
2	5.82	0.10	22.01	0.12	0.23	0.01	1.77	0.01	4.15	0.02	0.56	0.02	0.07	0.00	3.18	0.02	62.01	0.18
3	6.20	0.11	17.82	0.11	0.06	0.01	0.76	0.01	7.90	0.04	0.38	0.01	0.18	0.01	8.76	0.05	57.72	0.22
3	6.31	0.11	18.13	0.11	0.12	0.01	0.99	0.01	7.03	0.04	0.39	0.01	0.18	0.01	8.71	0.05	57.93	0.21
3	6.74	0.11	18.81	0.11	0.17	0.01	1.80	0.01	5.90	0.03	0.38	0.01	0.14	0.01	7.17	0.04	58.67	0.21
3	5.07	0.11	15.88	0.11	0.18	0.01	1.66	0.01	4.58	0.03	0.52	0.01	0.17	0.01	8.74	0.05	62.97	0.21
3	5.46	0.11	18.75	0.12	0.15	0.01	2.00	0.01	3.50	0.02	0.53	0.01	0.12	0.00	6.61	0.04	62.67	0.20
3	6.47	0.11	16.60	0.10	ND	ND	0.29	0.01	16.89	0.08	0.17	0.01	0.06	0.00	2.29	0.02	57.06	0.20
3	5.66	0.10	15.68	0.10	ND	ND	0.45	0.01	12.95	0.06	0.89	0.02	0.17	0.01	8.99	0.05	55.04	0.22
3	6.40	0.11	19.55	0.12	0.10	0.01	2.29	0.02	5.66	0.03	0.50	0.02	0.13	0.01	6.66	0.04	58.48	0.21
3	6.55	0.11	17.66	0.11	0.08	0.01	0.90	0.01	6.26	0.03	0.46	0.01	0.17	0.01	6.39	0.04	61.34	0.21
3	6.47	0.11	18.24	0.11	0.15	0.01	1.18	0.01	7.12	0.04	0.51	0.02	0.14	0.01	6.63	0.04	59.33	0.21
3	6.56	0.11	18.63	0.12	0.07	0.01	0.88	0.01	7.48	0.04	0.49	0.02	0.13	0.01	6.47	0.04	59.09	0.21
4	6.02	0.15	20.00	0.14	0.07	0.01	2.59	0.02	2.37	0.02	0.38	0.01	0.14	0.01	6.59	0.04	61.60	0.22
4	6.14	0.11	19.82	0.12	0.10	0.01	2.57	0.02	2.33	0.02	0.32	0.01	0.13	0.01	7.16	0.04	61.18	0.20
4	6.59	0.11	22.31	0.13	0.04	0.01	2.45	0.02	2.18	0.02	0.44	0.01	0.12	0.00	5.92	0.04	59.74	0.20
4	6.07	0.11	20.78	0.12	0.07	0.01	1.96	0.01	1.97	0.01	0.39	0.01	0.13	0.00	6.75	0.04	61.64	0.20
4	5.19	0.11	18.73	0.12	0.08	0.01	1.48	0.01	2.33	0.02	0.43	0.01	0.14	0.01	7.75	0.05	63.66	0.21
4	6.11	0.11	20.66	0.12	0.10	0.01	1.33	0.01	6.22	0.03	0.39	0.01	0.10	0.00	5.54	0.03	59.33	0.20
4	6.42	0.10	17.34	0.10	ND	ND	0.54	0.01	13.94	0.07	0.33	0.01	0.11	0.01	6.14	0.04	54.97	0.21
4	5.60	0.11	18.72	0.12	0.07	0.01	1.27	0.01	3.97	0.02	0.56	0.01	0.15	0.01	7.54	0.05	61.92	0.20
4	6.10	0.11	20.63	0.12	0.06	0.01	1.62	0.01	3.25	0.02	0.44	0.01	0.13	0.00	6.46	0.04	61.08	0.20
4	6.48	0.11	21.00	0.12	0.07	0.01	2.68	0.02	3.01	0.02	0.35	0.01	0.12	0.00	6.53	0.04	59.53	0.20

Continuation of table B12

	Al	Al +/-	Si	Si +/-	P	P +/-	K	K +/-	Ca	Ca +/-	Ti	Ti +/-	Mn	Mn +/-	Fe	Fe +/-	LE	LE +/-
4	6.18	0.11	19.58	0.12	ND	ND	1.99	0.01	3.92	0.02	0.35	0.01	0.17	0.01	7.84	0.04	59.75	0.20
4	6.75	0.11	20.08	0.12	0.04	0.01	1.95	0.01	4.14	0.02	0.36	0.01	0.13	0.01	6.62	0.04	59.69	0.20
5	4.70	0.11	18.70	0.13	0.10	0.01	1.15	0.01	2.85	0.02	0.55	0.02	0.13	0.01	6.80	0.05	64.82	0.21
5	4.61	0.11	20.22	0.14	0.08	0.01	0.90	0.01	2.91	0.02	0.38	0.01	0.10	0.00	5.26	0.04	65.35	0.21
5	4.61	0.10	19.52	0.13	0.20	0.01	0.13	0.01	2.48	0.02	0.44	0.01	0.45	0.01	9.17	0.05	62.83	0.21
5	5.01	0.10	20.81	0.13	0.13	0.01	0.08	0.01	2.55	0.02	0.37	0.01	0.11	0.00	6.62	0.04	64.16	0.19
5	5.38	0.10	17.21	0.10	0.09	0.01	ND	ND	14.76	0.07	0.50	0.02	0.13	0.01	7.33	0.04	54.43	0.21
5	5.42	0.10	17.19	0.10	ND	ND	ND	ND	14.94	0.07	0.57	0.02	0.12	0.01	6.43	0.04	55.15	0.21
5	5.62	0.10	19.67	0.11	0.06	0.01	0.48	0.01	8.34	0.04	0.34	0.01	0.10	0.00	6.32	0.04	58.90	0.19
5	4.85	0.10	24.84	0.13	0.10	0.01	1.92	0.01	2.23	0.01	0.34	0.01	0.10	0.00	5.57	0.03	59.84	0.19
5	5.43	0.10	22.27	0.13	0.12	0.01	0.80	0.01	2.64	0.02	0.54	0.01	0.26	0.01	7.64	0.04	60.12	0.20
5	5.00	0.10	20.76	0.12	0.15	0.01	0.76	0.01	2.46	0.02	0.48	0.01	0.18	0.01	8.05	0.05	61.98	0.20
5	5.27	0.10	21.26	0.12	0.15	0.01	0.96	0.01	3.22	0.02	0.40	0.01	0.15	0.01	8.10	0.05	60.27	0.20

Table B13: The table presents the data of the cross-section from the XRF-analysis of the alterations at locality D. The elements are given in wt.% with their respective standard error. ND is an abbreviation for "No Data".

XRF-measurements of alterations at Locality D

Alteration	wt.% element																	
nr	Al	Al +/-	Si	Si +/-	Cl	Cl +/-	K	K +/-	Ca	Ca +/-	Ti	Ti +/-	Mn	Mn +/-	Fe	Fe +/-	LE	LE +/-
1	3.59	0.10	15.19	0.11	ND	ND	2.72	0.02	3.08	0.02	0.16	0.01	0.06	0.00	3.37	0.03	71.64	0.18
1	3.10	0.10	13.50	0.10	ND	ND	2.29	0.02	3.17	0.02	0.22	0.01	0.07	0.00	3.68	0.03	73.76	0.17
1	3.32	0.10	13.05	0.10	ND	ND	3.46	0.02	3.36	0.02	0.16	0.01	0.06	0.00	3.19	0.02	73.17	0.17
1	2.77	0.11	12.93	0.10	ND	ND	4.54	0.03	1.83	0.02	0.21	0.01	0.06	0.00	3.11	0.03	74.36	0.18
1	3.08	0.11	12.25	0.10	ND	ND	4.96	0.03	2.05	0.02	0.19	0.01	0.08	0.00	4.09	0.03	73.07	0.18
1	2.69	0.11	11.65	0.09	ND	ND	5.47	0.03	2.16	0.02	0.12	0.01	0.08	0.00	3.79	0.03	73.85	0.18
1	2.82	0.11	13.03	0.10	ND	ND	4.92	0.03	1.89	0.02	0.18	0.01	0.06	0.00	3.02	0.02	73.87	0.17
1	2.71	0.10	12.92	0.10	ND	ND	4.05	0.03	2.87	0.02	0.19	0.01	0.05	0.00	2.74	0.02	74.26	0.17
1	2.91	0.10	13.45	0.10	ND	ND	2.32	0.02	2.92	0.02	0.19	0.01	0.06	0.00	3.36	0.02	74.56	0.16
1	2.50	0.09	15.41	0.11	ND	ND	2.69	0.02	2.80	0.02	0.13	0.01	0.05	0.00	2.65	0.02	73.57	0.16
1	3.18	0.10	13.31	0.10	ND	ND	3.55	0.02	3.68	0.02	0.18	0.01	0.07	0.00	3.35	0.03	72.45	0.18
2	2.23	0.10	10.60	0.09	ND	ND	3.83	0.03	2.01	0.02	0.14	0.01	0.05	0.00	2.36	0.02	78.55	0.16
2	1.30	0.09	7.21	0.07	ND	ND	2.55	0.02	1.61	0.01	0.11	0.01	0.05	0.00	2.39	0.02	84.59	0.13
2	1.02	0.09	4.54	0.05	2.86	0.16	2.65	0.02	1.87	0.01	0.11	0.01	0.05	0.00	2.14	0.02	84.56	0.19
2	1.85	0.10	8.22	0.12	ND	ND	2.83	0.04	1.61	0.02	0.15	0.01	0.10	0.00	2.76	0.04	79.73	0.85
2	0.75	0.08	5.66	0.06	2.88	0.17	2.23	0.02	2.33	0.02	0.10	0.01	0.07	0.00	1.90	0.02	83.89	0.19
2	1.64	0.09	8.58	0.08	ND	ND	2.57	0.02	4.48	0.03	0.15	0.01	0.08	0.00	2.51	0.02	79.79	0.14
2	1.73	0.11	8.08	0.09	ND	ND	2.66	0.02	1.18	0.01	0.14	0.01	0.07	0.00	2.50	0.02	83.45	0.16
2	1.74	0.10	10.14	0.10	ND	ND	1.62	0.02	2.37	0.02	0.16	0.01	0.07	0.00	3.21	0.03	80.48	0.16

Continuation of table B13

	Al	Al +/-	Si	Si +/-	Cl	Cl +/-	K	K +/-	Ca	Ca +/-	Ti	Ti +/-	Mn	Mn +/-	Fe	Fe +/-	LE	LE +/-
2	1.06	0.09	8.44	0.09	ND	ND	0.86	0.01	2.74	0.02	0.10	0.01	0.06	0.00	2.34	0.02	84.23	0.14
2	2.00	0.10	8.65	0.09	ND	ND	1.07	0.01	5.97	0.04	0.11	0.01	0.09	0.00	3.93	0.03	77.96	0.17
2	1.54	0.08	12.77	0.09	ND	ND	0.90	0.01	3.95	0.02	0.13	0.01	0.06	0.00	2.76	0.02	77.69	0.14

Table B14: The table presents the data of the cross-section from the XRF-analysis of the alterations at locality E. The elements are given in wt.% with their respective standard error. ND is an abbreviation for "No Data".

XRF-measurements of alterations at Locality E

Alteration	wt.% element																	
nr	Mg	Mg +/-	Al	Al +/-	Si	Si +/-	K	K +/-	Ca	Ca +/-	Ti	Ti +/-	Mn	Mn +/-	Fe	Fe +/-	LE	LE +/-
1	ND	ND	2.38	0.09	13.82	0.10	0.99	0.01	2.56	0.02	0.24	0.01	0.07	0.00	3.44	0.02	76.31	0.15
1	ND	ND	2.59	0.09	15.61	0.11	0.94	0.01	2.76	0.02	0.20	0.01	0.06	0.00	2.92	0.02	74.72	0.16
1	ND	ND	2.72	0.09	16.53	0.11	1.20	0.01	2.75	0.02	0.13	0.01	0.05	0.00	2.47	0.02	74.00	0.16
1	ND	ND	2.42	0.09	14.97	0.10	1.52	0.01	2.84	0.02	0.12	0.01	0.03	0.00	1.50	0.01	76.44	0.15
1	ND	ND	2.92	0.09	16.78	0.11	2.25	0.02	2.70	0.02	0.19	0.01	0.06	0.00	3.02	0.02	71.88	0.16
1	ND	ND	2.76	0.09	13.87	0.10	1.84	0.01	3.37	0.02	0.27	0.01	0.09	0.00	5.22	0.03	72.36	0.16
1	ND	ND	3.17	0.09	16.58	0.11	2.51	0.02	2.38	0.02	0.28	0.01	0.07	0.00	4.43	0.03	70.33	0.17
1	ND	ND	3.00	0.10	15.58	0.11	2.41	0.02	1.93	0.01	0.20	0.01	0.05	0.00	2.92	0.02	73.71	0.16
1	ND	ND	2.92	0.09	14.47	0.10	1.45	0.01	2.73	0.02	0.24	0.01	0.09	0.00	4.90	0.03	73.00	0.17
1	ND	ND	3.63	0.10	15.81	0.11	1.47	0.01	3.24	0.02	0.24	0.01	0.07	0.00	4.07	0.03	71.26	0.17
1	ND	ND	2.65	0.10	13.49	0.11	0.75	0.01	3.37	0.02	0.21	0.01	0.05	0.00	3.07	0.02	76.23	0.17
2	ND	ND	2.85	0.09	14.49	0.10	0.78	0.01	3.50	0.02	0.20	0.01	0.05	0.00	3.05	0.02	74.88	0.16
2	ND	ND	2.77	0.09	16.12	0.11	1.22	0.01	2.99	0.02	0.31	0.01	0.10	0.00	4.95	0.03	71.32	0.17
2	ND	ND	3.52	0.09	18.62	0.11	1.53	0.01	3.51	0.02	0.15	0.01	0.04	0.00	1.81	0.02	70.61	0.16
2	ND	ND	3.01	0.09	15.69	0.11	2.05	0.02	3.13	0.02	0.25	0.01	0.08	0.00	3.83	0.03	71.75	0.17
2	ND	ND	2.41	0.09	14.07	0.11	1.93	0.02	2.85	0.02	0.26	0.01	0.08	0.00	4.31	0.03	73.88	0.17
2	ND	ND	2.50	0.10	11.30	0.09	1.47	0.01	6.10	0.04	0.24	0.01	0.08	0.00	4.25	0.03	73.83	0.18
2	ND	ND	2.75	0.09	15.58	0.10	2.11	0.01	2.17	0.01	0.24	0.01	0.06	0.00	2.90	0.02	73.99	0.16
2	ND	ND	0.76	0.10	7.86	0.09	1.24	0.01	1.66	0.02	0.20	0.01	0.06	0.00	3.59	0.03	84.40	0.16
2	ND	ND	2.17	0.10	13.13	0.11	1.16	0.01	2.57	0.02	0.24	0.01	0.08	0.00	4.32	0.03	76.05	0.17

Continuation of table B14

	Mg	Mg +/-	Al	Al +/-	Si	Si +/-	K	K +/-	Ca	Ca +/-	Ti	Ti +/-	Mn	Mn +/-	Fe	Fe +/-	LE	LE +/-
2	ND	ND	3.67	0.10	16.58	0.11	1.82	0.01	2.99	0.02	0.26	0.01	0.07	0.00	4.40	0.03	69.93	0.18
2	2.28	0.75	3.66	0.10	15.08	0.15	1.49	0.02	2.77	0.03	0.31	0.01	0.09	0.00	5.25	0.05	68.81	0.56
3	ND	ND	2.41	0.09	13.21	0.10	0.70	0.01	3.73	0.02	0.25	0.01	0.07	0.00	3.83	0.03	75.64	0.16
3	ND	ND	2.51	0.09	13.87	0.10	0.76	0.01	3.20	0.02	0.22	0.01	0.05	0.00	2.63	0.02	76.58	0.16
3	ND	ND	2.62	0.09	15.25	0.11	1.02	0.01	2.93	0.02	0.30	0.01	0.08	0.00	4.39	0.03	73.16	0.17
3	ND	ND	3.03	0.09	16.02	0.11	1.47	0.01	3.51	0.02	0.21	0.01	0.05	0.00	2.92	0.02	72.60	0.16
3	ND	ND	2.02	0.08	13.89	0.10	1.13	0.01	2.85	0.02	0.32	0.01	0.07	0.00	4.14	0.03	75.37	0.15
3	ND	ND	2.55	0.10	15.69	0.12	2.49	0.02	4.22	0.03	0.16	0.01	0.04	0.00	1.96	0.02	72.71	0.18
3	ND	ND	2.09	0.11	12.17	0.12	2.00	0.02	4.10	0.03	0.25	0.01	0.06	0.00	3.68	0.03	75.45	0.20
3	ND	ND	1.48	0.14	10.30	0.22	1.50	0.03	3.78	0.08	0.24	0.02	0.05	0.00	3.34	0.07	75.19	1.36
3	ND	ND	1.93	0.12	11.62	0.12	1.86	0.02	4.75	0.04	0.29	0.02	0.10	0.01	5.69	0.05	73.53	0.23
3	ND	ND	2.48	0.10	12.02	0.15	1.09	0.01	3.31	0.04	0.27	0.01	0.10	0.00	5.33	0.06	72.74	0.69
3	ND	ND	3.57	0.10	16.29	0.12	1.72	0.01	3.00	0.02	0.25	0.01	0.06	0.00	3.28	0.03	71.62	0.18
4	ND	ND	2.88	0.09	15.41	0.11	0.82	0.01	3.82	0.02	0.35	0.01	0.11	0.00	5.78	0.04	70.55	0.18
4	ND	ND	3.41	0.09	15.68	0.10	1.54	0.01	3.37	0.02	0.21	0.01	0.06	0.00	3.18	0.02	72.34	0.16
4	ND	ND	3.31	0.09	17.78	0.11	1.63	0.01	2.55	0.02	0.30	0.01	0.07	0.00	4.03	0.03	70.12	0.17
4	ND	ND	3.53	0.09	18.87	0.11	2.07	0.01	2.75	0.02	0.26	0.01	0.06	0.00	3.16	0.02	69.11	0.17
4	ND	ND	2.61	0.09	18.56	0.12	1.60	0.01	4.61	0.03	0.16	0.01	0.05	0.00	2.59	0.02	69.62	0.17
4	ND	ND	3.90	0.10	16.65	0.11	2.45	0.02	6.89	0.04	0.20	0.01	0.04	0.00	2.51	0.02	67.14	0.18
4	ND	ND	3.12	0.10	16.72	0.12	1.40	0.01	4.63	0.03	0.27	0.01	0.09	0.00	4.46	0.03	69.11	0.19
4	ND	ND	2.97	0.09	19.96	0.13	1.09	0.01	4.84	0.03	0.17	0.01	0.05	0.00	2.61	0.02	68.13	0.18
4	ND	ND	3.13	0.09	16.93	0.11	1.16	0.01	3.61	0.02	0.31	0.01	0.09	0.00	4.96	0.03	69.58	0.18
4	ND	ND	2.66	0.09	16.07	0.11	0.97	0.01	3.18	0.02	0.19	0.01	0.06	0.00	3.26	0.02	73.40	0.17

Continuation of table B14

	Mg	Mg +/-	Al	Al +/-	Si	Si +/-	K	K +/-	Ca	Ca +/-	Ti	Ti +/-	Mn	Mn +/-	Fe	Fe +/-	LE	LE +/-
4	ND	ND	3.42	0.09	20.12	0.12	1.87	0.01	4.36	0.02	0.23	0.01	0.04	0.00	2.42	0.02	67.33	0.17
5	ND	ND	3.76	0.09	24.47	0.13	1.35	0.01	3.06	0.02	0.24	0.01	0.07	0.00	3.37	0.02	63.46	0.18
5	ND	ND	4.33	0.10	20.42	0.12	0.84	0.01	4.03	0.02	0.32	0.01	0.09	0.00	5.23	0.03	64.45	0.19
5	ND	ND	4.59	0.10	21.38	0.12	2.05	0.01	4.01	0.02	0.30	0.01	0.07	0.00	4.17	0.03	63.14	0.19
5	ND	ND	4.08	0.09	25.84	0.14	1.70	0.01	3.45	0.02	0.20	0.01	0.05	0.00	2.45	0.02	61.92	0.18
5	ND	ND	3.67	0.09	24.95	0.13	1.83	0.01	3.47	0.02	0.26	0.01	0.08	0.00	4.64	0.03	60.81	0.18
5	ND	ND	4.45	0.09	28.13	0.13	4.06	0.02	3.46	0.02	0.25	0.01	0.06	0.00	3.39	0.02	55.88	0.19
5	ND	ND	5.10	0.10	23.41	0.13	1.92	0.01	3.59	0.02	0.23	0.01	0.05	0.00	3.19	0.02	62.23	0.18
5	ND	ND	4.68	0.10	27.86	0.15	1.49	0.01	3.40	0.02	0.19	0.01	0.04	0.00	2.64	0.02	59.52	0.20
5	ND	ND	3.30	0.09	20.88	0.13	0.59	0.01	3.56	0.02	0.30	0.01	0.09	0.00	5.00	0.03	66.01	0.19
5	ND	ND	3.57	0.09	21.05	0.13	0.59	0.01	3.90	0.02	0.27	0.01	0.08	0.00	4.17	0.03	66.14	0.19
5	ND	ND	3.94	0.09	27.25	0.14	0.59	0.01	3.43	0.02	0.22	0.01	0.07	0.00	3.48	0.02	60.87	0.18

Table B15: The table presents the data of the cross-section from the XRF-analysis of the alterations at locality F. The elements are given in wt.% with their respective standard error. ND is an abbreviation for "No Data".

XRF-measurements of alterations at Locality F

Alteration	wt.% element																			
nr	Mg	Mg +/-	Al	Al +/-	Si	Si +/-	Cl	Cl +/-	K	K +/-	Ca	Ca +/-	Ti	Ti +/-	Mn	Mn +/-	Fe	Fe +/-	LE	LE +/-
1	3.17	0.92	2.04	0.09	12.05	0.15	ND	ND	0.55	0.01	2.40	0.03	0.11	0.01	0.04	0.00	1.86	0.02	77.57	0.75
1	ND	ND	1.49	0.08	8.36	0.08	ND	ND	0.68	0.01	2.42	0.02	0.20	0.01	0.07	0.00	3.76	0.03	82.82	0.13
1	ND	ND	1.69	0.08	6.86	0.07	ND	ND	0.76	0.01	2.73	0.02	0.22	0.01	0.11	0.00	5.57	0.04	81.79	0.14
1	ND	ND	2.51	0.09	7.35	0.07	ND	ND	1.01	0.01	3.11	0.02	0.24	0.01	0.07	0.00	3.97	0.03	81.52	0.15
1	ND	ND	1.59	0.08	6.98	0.07	ND	ND	0.87	0.01	2.22	0.02	0.19	0.01	0.06	0.00	3.26	0.03	84.64	0.13
1	ND	ND	1.51	0.09	9.13	0.08	ND	ND	1.92	0.01	2.03	0.02	0.17	0.01	0.06	0.00	2.93	0.02	82.05	0.14
1	ND	ND	1.47	0.08	6.02	0.06	1.89	0.16	1.25	0.01	2.86	0.02	0.34	0.01	0.12	0.00	5.54	0.04	80.25	0.20
1	ND	ND	1.20	0.08	6.58	0.07	1.55	0.17	0.74	0.01	1.98	0.02	0.27	0.01	0.07	0.00	4.10	0.03	83.32	0.19
1	ND	ND	1.41	0.08	8.27	0.08	ND	ND	0.57	0.01	2.62	0.02	0.15	0.01	0.05	0.00	2.63	0.02	84.10	0.13
1	ND	ND	1.01	0.07	5.28	0.07	3.37	0.16	0.49	0.01	2.70	0.03	0.14	0.01	0.04	0.00	1.76	0.02	82.96	0.76
1	ND	ND	0.80	0.07	5.42	0.06	2.38	0.16	0.57	0.01	3.13	0.02	0.20	0.01	0.07	0.00	3.46	0.03	83.77	0.18
2	ND	ND	0.70	0.06	3.36	0.05	5.07	0.15	0.51	0.01	2.57	0.02	0.14	0.01	0.06	0.00	2.65	0.02	84.77	0.17
2	ND	ND	0.56	0.06	3.00	0.04	5.80	0.15	0.48	0.01	2.25	0.02	0.16	0.01	0.05	0.00	2.50	0.02	85.03	0.17
2	ND	ND	0.81	0.07	3.79	0.05	4.53	0.15	0.57	0.01	2.64	0.02	0.13	0.01	0.05	0.00	2.16	0.02	85.15	0.17
2	ND	ND	1.19	0.07	5.74	0.06	1.61	0.15	0.72	0.01	2.66	0.02	0.20	0.01	0.08	0.00	4.12	0.03	83.46	0.18
2	ND	ND	1.33	0.08	5.21	0.06	2.45	0.16	1.61	0.01	2.85	0.02	0.23	0.01	0.05	0.00	2.58	0.02	83.48	0.18
2	ND	ND	0.96	0.07	4.18	0.05	3.66	0.15	1.32	0.01	2.42	0.02	0.16	0.01	0.06	0.00	3.04	0.02	84.01	0.17
2	ND	ND	0.51	0.06	2.53	0.04	6.10	0.14	0.62	0.01	2.01	0.02	0.24	0.01	0.09	0.00	4.57	0.03	83.11	0.17
2	ND	ND	0.38	0.06	3.04	0.04	5.38	0.15	0.42	0.01	1.85	0.01	0.19	0.01	0.06	0.00	2.78	0.02	85.71	0.17

Continuation of table B15

	Mg	Mg +/-	Al	Al +/-	Si	Si +/-	Cl	Cl +/-	K	K +/-	Ca	Ca +/-	Ti	Ti +/-	Mn	Mn +/-	Fe	Fe +/-	LE	LE +/-
2	ND	ND	0.76	0.07	4.33	0.06	3.81	0.15	0.49	0.01	2.21	0.03	0.18	0.01	0.05	0.00	3.18	0.04	82.42	0.76
2	ND	ND	0.58	0.06	4.25	0.06	4.33	0.16	0.41	0.01	1.97	0.02	0.12	0.01	0.05	0.00	2.02	0.03	83.49	0.79
2	ND	ND	0.86	0.07	4.65	0.06	3.19	0.17	0.44	0.01	2.41	0.02	0.10	0.01	0.04	0.00	1.74	0.02	86.40	0.19

Appendix C Petrographic analysis results

Table C1: *The point count results are presented as the amount of points counted for each mineral along with the percentage out of the total points of 500. The standard error represents the error of the point counting process as presented by [Plas and Tobi, 1965].*

Thin section	Mineral	Points	Percentage	SE
A-1	Hbl	150	30	4.10
	Plag	311	62.20	4.34
	Chl	15	3	1.53
	Bt	2	0.40	0.56
	Qz	10	2	1.25
	Gt	0	0	0
	Other	12	2.40	1.37
A-2	Hbl	162	32.40	4.19
	Plag	289	57.80	4.42
	Chl	2	0.40	0.56
	Bt	29	5.80	2.09
	Qz	18	3.60	1.67
	Gt	0	0	0
	Other	0	0	0
A-3	Hbl	162	32.40	4.19
	Plag	287	57.40	4.42
	Chl	9	1.80	1.19
	Bt	22	4.40	1.83
	Qz	20	4	1.75
	Gt	0	0	0
	Other	0	0	0
B-1	Hbl	36	7.20	2.31
	Plag	286	57.20	4.43
	Chl	21	4.20	1.79
	Bt	1	0.20	0.40
	Qz	74	14.80	3.18
	Gt	14	2.80	1.48
	Other	68	13.60	3.07
B-2	Hbl	45	9	2.56
	Plag	252	50.40	4.47
	Chl	35	7	2.28
	Bt	5	1	0.89
	Qz	88	17.60	3.41
	Gt	0	0	0
	Other	65	13	3.01

Continuation of table C1

Thin section	Mineral	Points	Percentage	SE
C-1	Hbl	0	0	0
	Plag	240	48	4.47
	Chl	6	1.20	0.97
	Bt	159	31.80	4.17
	Qz	42	8.40	2.48
	Gt	53	10.60	2.75
	Other	0	0	0
C-2	Hbl	97	19.40	3.54
	Plag	260	52	4.47
	Chl	0	0	0
	Bt	78	15.60	3.25
	Qz	22	4.40	1.83
	Gt	43	8.60	2.51
	Other	0	0	0
C-3	Hbl	153	30.60	4.12
	Plag	269	53.80	4.46
	Chl	14	2.80	1.48
	Bt	15	3	1.53
	Qz	40	8	2.43
	Gt	9	1.80	1.19
	Other	0	0	0
C-4	Hbl	13	2.60	1.42
	Plag	227	45.40	4.45
	Chl	0	0	0
	Bt	117	23.40	3.79
	Qz	76	15.20	3.21
	Gt	62	12.40	2.95
	Other	5	1.00	0.89
D-1	Hbl	0	0	0
	Plag	241	48.20	4.47
	Chl	0	0	0
	Bt	69	13.80	3.08
	Qz	187	37.40	4.33
	Gt	0	0	0
	Other	3	0.60	0.69

Continuation of table C1

Thin section	Mineral	Points	Percentage	SE
D-2	Hbl	0	0	0
	Plag	214	42.80	4.43
	Chl	3	0.60	0.69
	Bt	97	19.40	3.54
	Qz	165	33.00	4.21
	Gt	0	0	0
	Other	21	4.20	1.79
E-1	Hbl	30	6.00	2.12
	Plag	260	52.00	4.47
	Chl	0	0	0
	Bt	63	12.60	2.97
	Qz	146	29.20	4.07
	Gt	0	0	0
	Other	1	0.20	0.40
E-2	Hbl	28	5.60	2.06
	Plag	308	61.60	4.35
	Chl	0	0	0
	Bt	76	15.20	3.21
	Qz	88	17.60	3.41
	Gt	0	0	0
	Other	0	0	0
F-1	Hbl	46	9.20	2.59
	Plag	286	57.20	4.43
	Chl	0	0	0
	Bt	89	17.80	3.42
	Qz	79	15.80	3.26
	Gt	0	0	0
	Other	0	0	0
F-2	Hbl	52	10.40	2.73
	Plag	227	45.40	4.45
	Chl	0	0	0
	Bt	98	19.60	3.55
	Qz	121	24.20	3.83
	Gt	0	0	0
	Other	1	0.20	0.40

Continuation of table C1

Thin section	Mineral	Points	Percentage	SE
A-4a	Hbl	54	10.80	2.78
	Plag	107	21.40	3.67
	Chl	11	2.20	1.31
	Bt	7	1.40	1.05
	Qz	7	1.40	1.05
	Gt	298	59.60	4.39
	Other	16	3.20	1.57
A-4b	Hbl	1	0.20	0.40
	Plag	15	3	1.53
	Chl	3	0.60	0.69
	Bt	0	0	0
	Qz	9	1.80	1.19
	Gt	469	93.80	2.16
	Other	3	0.60	0.69

Table C2: *The angles measured for the Michel-Levy analysis are provided in the following table. The maximum average between two angles were used for the localities' respective max. extinction angle.*

Locality	Angles measured		Average
	α_1	α_2	
A	8	9	8.5
	6	8	7
	10	12	11
	12	15	13.5
	10	8	9
	10	7	8.5
	9	7	8
B	8	7	7.5
	9	7	8
	6	5	5.5
	8	6	7
	8	5	6.5
C	9	13	11
	16	18	17
	12	10	11
	20	24	22
	10	15	12.5
	26	24	25
	16	16	16
	23	23	23
D	13	15	14
E	21	23	22
	14	18	16
	23	26	2.5
	25	25	25
	20	25	22.5
	16	19	17.5
	28	26	27
F	15	20	17.5
	17	20	18,5
	18	22	20
	12	14	13
	15	13	14